

國立臺灣大學理學院心理學研究所



碩士論文

Graduate Institute of Psychology

College of Science

National Taiwan University

Master Thesis

知覺群聚中的多重色彩機制

Multiple Color Mechanisms for Perceptual Grouping

林立

Lee Lin


指導教授：陳建中 博士

Advisor: Chien-Chung Chen, Ph.D.

中華民國 109 年 7 月

July 2020

## 摘要



本研究探討知覺群聚 (perceptual grouping) 中色彩視覺機制 (color vision mechanisms) 的調頻 (tuning) 與反應 (response) 特性。實驗材料由數組隨機分布於影像中的「三點」 (tripole) 組成，定錨點 (anchor dot) 決定每組三點的隨機位置，另外兩個周邊點 (context dots) 的位置取決於其與定錨點位置間的幾何關係。若將定錨點與其中一個周邊點組合在一起，觀察者可能看到順時針或逆時針螺旋形狀的整體圖形。定錨點的色度 (chromaticity) 均勻分布在色彩空間中的等亮度平面 (equiluminant plane) 上，其中一個周邊點的色度和定錨點色度相同，另一個周邊點色度相對於定錨點色度變化。兩個周邊點的色彩對比 (color contrast) 落於一至四倍該色度之偵測閾值 (detection threshold) 範圍間。受試者回答看到的實驗刺激為順時針或逆時針螺旋圖形。結果顯示，將定錨點與其一周邊點組合在一起的機率隨著該周邊點的色彩對比上升而上升，但隨著另一周邊點的色彩對比上升而下降，暗示兩種組合方式互相競爭觀察者的圖形覺知 (percept)。無論定錨點色度，將定錨點與周邊點組合的機率隨著兩點間的色度差異增加而下降。包含四組色彩機制的除法抑制模型 (divisive inhibition model) 可解釋上述觀察現象，其中兩組色彩機制的調頻函數 (tuning functions) 與過去文獻中的紅綠 (L-M) 及藍黃 (S-[L-M]) 機制相似，另外兩組則偏好其他中間顏色。此研究指出知覺群聚中涉及紅綠與藍黃以外的色彩機制。

**關鍵詞：**知覺群聚、色彩機制、除法抑制、色彩調頻

# Multiple Color Mechanisms for Perceptual Grouping

Lee Lin



## Abstract

This study investigated the tuning and response properties of the color vision mechanisms in perceptual grouping using tripole Glass patterns. A tripole Glass pattern consists of randomly-distributed groups of three dots, with one anchor dot and two context dots. The geometric relationship between any two dots defines the perceived global pattern. Observers may perceive either a clockwise (CW) or counter-clockwise (CCW) spiral if they can locally match the anchor dot with one or the other context dot, respectively. The chromaticity of the anchor dot was equally distributed on the equiluminant plane of a color space. One context dot had the same chromaticity as the anchor dot, while the other varied in chromaticity. The contrast of each context dot varied between one- to four-fold the detection threshold of the corresponding chromaticity. The observer was asked to judge whether the pattern was a CW or a CCW spiral. The probability of grouping the anchor dot with one context dot increased as a sigmoid-shaped function of the context dot contrast. The probability function shifted in a downward right direction as the contrast of the other context dot increased, suggesting a competition between the two ways of grouping. The probability of grouping the anchor and a context dot also decreased as the chromaticity difference between the two dots increased regardless of the anchor dot chromaticity. A divisive inhibition model with four pairs of color mechanisms explained the result. The tuning functions of two pairs of these mechanisms were similar to those of the cardinal equiluminant mechanisms. The other two pairs of mechanisms preferred some intermediate colors.

We conclude that perceptual grouping involves extra color mechanisms than those found at the former stage of visual processing.

**Keywords:** perceptual grouping, chromatic mechanisms, divisive inhibition, color tuning

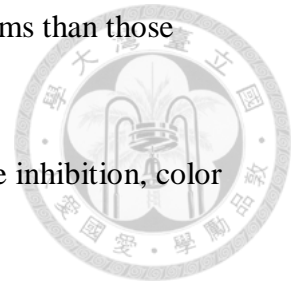
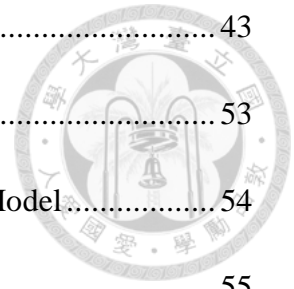


## Table of Contents



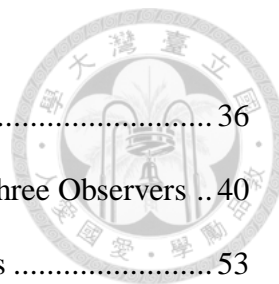
1. Introduction .....	1
2. Method .....	13
2.1. Participants .....	13
2.2. Apparatus .....	13
2.3. Stimulus .....	13
2.4. Procedure .....	16
3. Result.....	18
4. Discussion.....	23
4.1. The contrast effect on perceptual grouping.....	23
4.2. The role of gain control.....	23
4.3. The chromaticity effect on perceptual grouping .....	25
4.4. Modeling chromatic mechanisms.....	26
4.5. Model overview.....	29
4.6. The quantitative description of the model .....	29
4.7. Model implementation and performance .....	34
4.8. Tests on the number of chromatic mechanisms .....	35
4.9. Spectral sensitivity of the mechanisms .....	36
4.10. Comparisons to the literature .....	38
4.11. The issue of subjective equiluminance .....	40
5. Conclusion.....	42

6. References .....	43
Appendix A: Detection Threshold Measurement .....	53
Appendix B: Symbols Used in the Quantitative Description of the Model.....	54
Appendix C. Best-fitted Model Parameter List .....	55



## List of Tables

Table 1 Contrast Sensitivity of the Three Observers .....	36
Table 2 Polar Representation of the Estimated Mechanisms for the Three Observers ..	40
Table A1 Normalized Cone Contrast Vectors for the Three Observers .....	53
Table A2 Symbols Used in the Quantitative Description of the Model .....	54
Table A3 Best-fitted Model Parameters.....	55



## List of Figures

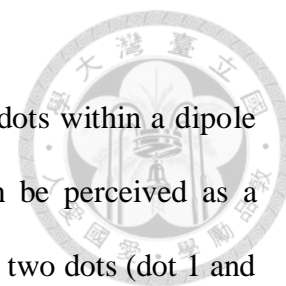
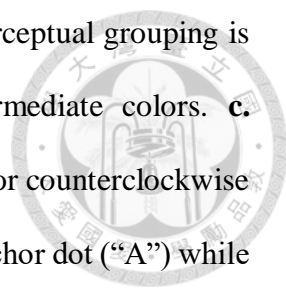


Figure 1. Examples of the geometric relationship between the two dots within a dipole and the resulting Glass patterns. **a.** A Glass pattern that can be perceived as a concentric pattern. The distance from the stimulus center to the two dots (dot 1 and dot 2) are the same. The virtual line connecting the stimulus center and dot 2 have an angle difference to the line connecting the center and dot 1. **b.** A Glass pattern that can be perceived as a spiral pattern. The distance from the stimulus center to dot 2 is larger than that to dot 1. The virtual line connecting the stimulus center and dot 2 have an angle difference to the line connecting the center and dot 1..... 5

Figure 2. A tripole Glass pattern and the geometric description of the dots within a tripole. **a.** An example of a tripole Glass pattern. **b.** An illustration of a local tripole. A tripole consists of three dots, with one anchor dot (“A”) and two context dots (“C” and “CC”). If the visual system organizes the anchor dot with one of the context dots and integrates the resulting dot pairs over space, the observer might perceive a clockwise (CW) or counterclockwise (CCW) spiral pattern. .... 8

Figure 3. Two hypotheses for the underlying color mechanisms. The central rows of **a** and **b** illustrate the mechanism and dot color directions. The thin black arrows are the preferred color directions of the color mechanisms. The thick blue, white, and pink arrows are the dot color directions. The bottom rows are the predictions from the hypotheses. The abscissa is the chromaticity difference between the anchor dot and the different color dot. The ordinate on the left is the probability of grouping the anchor dot with the same color dot,  $P(A+S)$ . The ordinate on the right side is the probability of grouping the anchor dot with the different color dot,  $P(A+D)$ . The blue and pink dashed lines mark the conditions illustrated in the central rows. **a.** Cardinal mechanisms hypothesis: perceptual grouping is supported by cardinal color





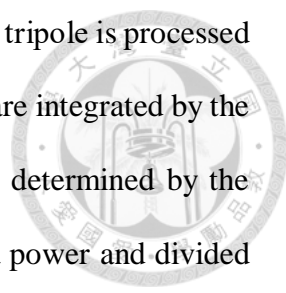
mechanisms alone. **b.** Intermediate mechanisms hypothesis: perceptual grouping is supported by additional mechanisms that prefer some intermediate colors. **c.** Illustration of the tripole. One context dot (either the clockwise or counterclockwise dot; denoted as “S”) would have the same chromaticity as the anchor dot (“A”) while the other context dot (“D”) varied in chromaticity. .... 10

Figure 4. The equiluminant plane. Azimuth ( $\phi$ ) is the polar angle from L-M axis to the direction of the color vector. Color contrast (C) is the length of the vector, or the distance from the origin to the end of the vector. Some color vectors used in the experiment were also illustrated (see stimulus settings for details). .... 15

Figure 5. Examples of the tripole Glass patterns. Upper row: context dot contrast variations. The clockwise (CW) dot contrast increases from the leftmost image to the rightmost image. The counterclockwise (CCW) dot contrast increases in the opposite direction. Lower row: CCW dot chromaticity variation. In these examples, CCW dot chromaticity differs from 45° anchor/CW dot chromaticity from -90° to +90°. The color vectors of the examples on the equiluminant plane are illustrated in Figure 4. .... 17

Figure 6. The probability of grouping the anchor dot and the same color dot under different contrast and chromaticity combinations. Each row shows one anchor (“A”) dot chromaticity. Each column shows the chromaticity difference between “A” dot and the different color (“D”) dot. The abscissa is the same color (“S”) dot contrast. The ordinate is the probability of grouping “A” and “S” dots. Different symbols and lines correspond to “D” dot contrast levels and the model fits. **a.** The observer LL. **b.** CPY. **c.** LYS. (Continued.) .... 19

Figure 7. A schematic diagram of the divisive inhibition model. The perceptual grouping process begins with local tripoles (“A” for anchor dot, “C” for clockwise dot, and



“CC” for counterclockwise dot). Any dot pair, or dipole, within a tripole is processed by color-spatial linear operators. Then, the operator excitations are integrated by the global pattern detector. The response of the pattern detector is determined by the divisive inhibition process in which the excitation is raised by a power and divided by the inhibition plus a constant. The responses of the chromatic mechanisms are summed according to the preferred pattern orientation of the detectors. Finally, the decision value is the difference between CW and CCW pattern responses. The process for a task-irrelevant concentric pattern is not shown explicitly in this illustration. .... 30

Figure 8. Spectral sensitivity functions of the estimated mechanisms for the three observers and the average. The black lines are the estimated sensitivity functions. The red and blue dashed lines plotted are the proposed red-green (RG) and blue-yellow (BY) mechanisms (Guth et al., 1980), respectively. The black dashed (2-degree eccentricity estimate) or dotted lines (10-degree eccentricity estimate; almost overlapping with the 2-degree estimate) are luminosity efficiency functions (CIE, 2006) that represent the luminance (LUM) mechanism. .... 37

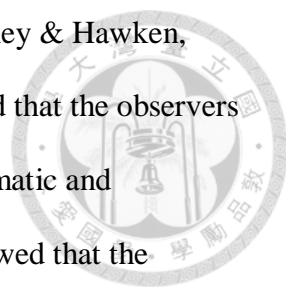
## 1. Introduction



One of the vision functions is the ability to recognize objects in an image. For this purpose, the visual system extracts important features from the spatial modulation of luminance and color of an image.

At the very beginning, an image elicits a response in the photoreceptors on the retina. Three types of photoreceptors are especially important under photopic conditions. These photoreceptors are referred to as long- (L-), medium- (M-), and short- (S-) wavelength sensitive cones according to their most sensitive range in the wavelength spectrum. Then, cone signals are sent to the lateral geniculate nucleus (LGN) through bipolar and ganglion cells. At the LGN, cone signals are linearly combined into three separate systems (Gegenfurtner & Kiper, 2003): one sums up L- and M-cone signals (L+M), one notes the difference between the L- and M-cone signals (L-M), and the other opposes S-cone to the sum of the L- and M-cone signals (S-[L+M]) (De Valois, Cottaris, Elfar, Mahon, & Wilson, 2000; Derrington, Krauskopf, & Lennie, 1984; Reid & Shapley, 2002). The first system is sensitive to luminance modulation while the latter two are sensitive to color variations. Accordingly, the first mechanism is referred to as the luminance mechanism, and the latter two are referred to as cone-opponent mechanisms, which are red-green and blue-yellow mechanisms despite that these mechanisms have nothing to do with color appearance. Finally, the signals are sent to the visual cortex.

Whilst earlier studies implied that the cone-opponent mechanisms were not involved in form perception (Livingstone & Hubel, 1988; Livingstone & Hubel, 1987; Zeki & Shipp, 1988), it is now widely accepted that the roles of these cone-opponent mechanisms in form perception are comparable with the luminance mechanism, albeit may have a slightly degraded performance (Friedman, Zhou, & von der Heydt, 2003;



Kiper, Fenstemaker, & Gegenfurtner, 1997; Moutoussis, 2015; Shapley & Hawken, 2011). For example, Webster, De Valois, and Switkes (1990) showed that the observers could discriminate the orientation or spatial frequency of both achromatic and equiluminant Gabor patches. Chen, Foley, and Brainard (2000a) showed that the observer could discriminate the target Gabor patch from the superimposed Gabor pedestal for achromatic and equiluminant stimuli, though the discrimination thresholds for chromatic stimuli were consistently higher than the threshold for achromatic stimuli. McIlhagga and Mullen (1996) generated a contour made up of aligned Gabor patches embedded in randomly-oriented Gabors, and found that the observer was equally able to detect the contour no matter whether the stimuli were achromatic or chromatic. These three mechanisms have been found to support many other pattern vision tasks, such as local pattern detection (Chen et al., 2000a; Chen, Foley, & Brainard, 2000b; Eskew, Newton, & Giulianini, 2001; Flanagan, Cavanagh, & Favreau, 1990; Giulianini & Eskew, 1998; Mullen & Losada, 1994; Mullen & Sankeralli, 1999; Poirson & Wandell, 1996; Sankeralli & Mullen, 1997), collinear facilitation (Ellenbogen, Polat, & Spitzer, 2006; Huang, Mullen, & Hess, 2007), contour integration (Beaudot & Mullen, 2000, 2001, 2003; Mullen, Beaudot, & McIlhagga, 2000), global pattern discrimination (Mullen & Beaudot, 2002), object detection (Hansen & Gegenfurtner, 2017), and others. The three mechanisms each tune to black-white, red-green, or blue-yellow contrast, respectively, are the most salient mechanisms, and are consistent with the physiological results of most post-receptoral ganglion and LGN cells, these mechanisms are referred to in the literature as cardinal mechanisms.

Although the cardinal mechanisms were prevalently found to support various kinds of visual tasks (Beaudot & Mullen, 2001, 2003; Chen et al., 2000a, 2000b; Ellenbogen et al., 2006; Eskew et al., 2001; Giulianini & Eskew, 1998; Huang et al., 2007; Mullen

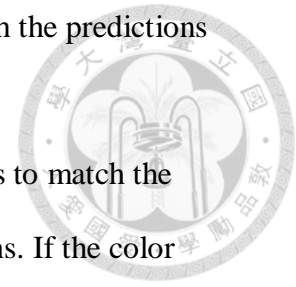
& Beaudot, 2002), some studies have shown results inconsistent with the predictions from the cardinal mechanisms.

For example, Webster and Mollon (1994) asked the participants to match the perceived color of a small disk after adapting to some color directions. If the color appearance was mediated by only cardinal mechanisms, adapting to the color directions that were intermediate to the cardinal directions should produce no color appearance change for all test colors on the color plane. However, they found that the perceived colors of the test stimuli shifted away from the adapting direction toward the orthogonal direction.

Nonetheless, this could be explained by the existence of additional color mechanisms, the intermediate mechanisms, which are most sensitive to intermediate color directions. Adapting to one intermediate direction reduced the sensitivity of the nearby intermediate mechanism, but not the other intermediate mechanism that preferred the orthogonal color direction. The adapted intermediate mechanisms would be much less activated while the orthogonal intermediate mechanism would remain similarly activated by the same color after, rather than before, the adaptation. Therefore, the perceived color shifted away from the adapting axis toward the orthogonal axis.

Cumulative studies have also suggested the existence of extra mechanisms other than the cardinal mechanisms in visual tasks, such as detection (D’Zmura & Knoblauch, 1998; Gegenfurtner & Kiper, 1992), discrimination (Zaidi & Halevy, 1993), collinear facilitation (Sato, Nagai, & Kuriki, 2020), tilt illusion (Clifford, Spehar, Solomon, Martin, & Qasim, 2003), image segregation (Hansen & Gegenfurtner, 2005, 2006, 2013), and others.

For example, Clifford et al. (2003) asked the observers to report the orientation of a sinusoidal grating surrounded by another tilted grating. They found that the strongest



tilt effect on the central grating occurred when the grating and the surrounding grating were the same color, no matter whether they were cardinal or intermediate colors. The intermediate color selectivity cannot simply be explained by the cardinal mechanisms.

To detect an object, the visual system integrates information from many neurons preferring different locations of the image. The process that integrates local elements into a global structure is called perceptual grouping. Wertheimer (1938) and other Gestalt psychologists studied perceptual grouping from a phenomenological aspect. They proposed grouping laws to describe how the local elements should be organized into a perceptual whole according to some element features or the relationship between the elements.

Among the grouping laws, the Law of Similarity describes how elements sharing similar features should be perceptually grouped. One such feature is color. Koffka (1963) demonstrated that the local elements can be organized by color similarity. Quinlan and Wilton (1998) measured the grouping strength of color similarity by comparing color similarity cues with other grouping cues, such as proximity. They used a row of colored elements. The central element was either similar in color (color similarity) or closer in position (proximity) to either the left or the right elements. The observers rated the strength of grouping the central element with the left or right elements. The grouping strength to either side was the strongest when proximity and color similarity cues favored the same organization, and the weakest when they conflicted. When the two grouping cues conflicted, half of the observers grouped the elements according to color similarity rather than proximity. This indicated that the observers could organize image elements by the color similarity of those elements, and that color similarity could be as an effective grouping cue as proximity in certain conditions.

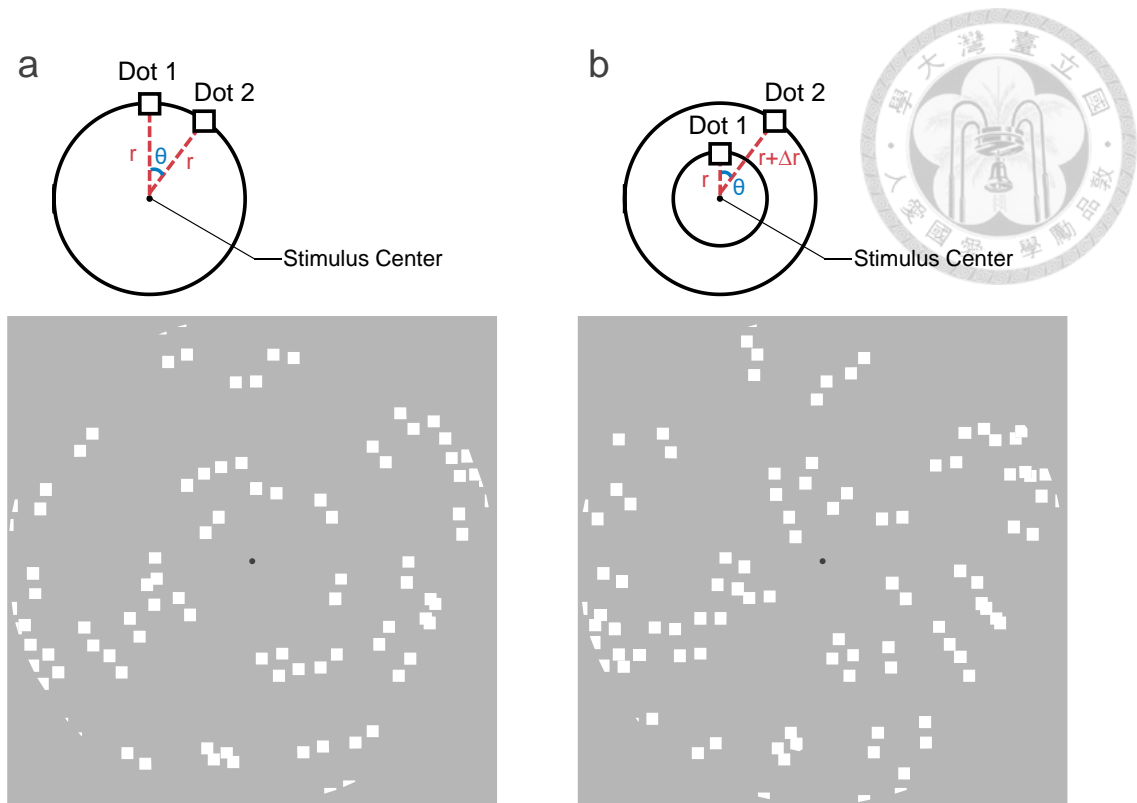


*Figure 1.* Examples of the geometric relationship between the two dots within a dipole and the resulting Glass patterns. **a.** A Glass pattern that can be perceived as a concentric pattern. The distance from the stimulus center to the two dots (dot 1 and dot 2) are the same. The virtual line connecting the stimulus center and dot 2 have an angle difference to the line connecting the center and dot 1. **b.** A Glass pattern that can be perceived as a spiral pattern. The distance from the stimulus center to dot 2 is larger than that to dot 1. The virtual line connecting the stimulus center and dot 2 have an angle difference to the line connecting the center and dot 1.

One paradigm in investigating perceptual grouping can be demonstrated with Glass patterns (Glass, 1969; Glass & Pérez, 1973; Glass & Switkes, 1976). A Glass pattern contains several dot pairs, or dipoles. These dipoles are randomly distributed in the image. A Glass pattern may appear to have a global structure if the dots within each dipole conform to some geometric relationship (Figure 1). The visual process of Glass patterns has two stages. At the first stage, two dots are organized into a dipole (Mandelli & Kiper, 2005; Wilson & Wilkinson, 1998; Wilson, Wilkinson, & Asaad, 1997; Wilson

& Switkes, 2005). At the second stage, dipoles are integrated over space into a global pattern (Chen, 2009; Dakin & Bex, 2001; Kurki, Laurinen, Peromaa, & Saarinen, 2003; Mandelli & Kiper, 2005; Wilson & Switkes, 2005; Wilson, Switkes, & De Valois, 2004). By manipulating the dot properties, such as luminance (Badcock, Clifford, & Khuu, 2005; Earle, 1999; Kurki et al., 2003; Lin, Cho, & Chen, 2017; Maloney, Mitchison, & Barlow, 1987; Prazdny, 1986; Wilson et al., 2004) and color (Cardinal & Kiper, 2003; Lin, 2016; Mandelli & Kiper, 2005; Wilson & Switkes, 2005), it is possible to build an understanding of the visual process for global form perception.

Investigating the role of color on perceptual grouping helps us to understand how the visual system integrates color information. Mandelli and Kiper (2005) focused on the color processing in the perceptual grouping of Glass patterns at the local stage. They manipulated the chromaticity of one dot and fixed that of the other dot within dipoles. Some dipoles were randomly oriented while others contributed to a concentric Glass pattern. They varied the proportion of the randomly oriented dipoles and measured the threshold of perceiving a concentric pattern. The result showed that the threshold increased as the chromaticity difference between the two dots increased, no matter whether the fixed chromaticity was in cardinal or intermediate color directions. This suggested that perceptual grouping at the local stage was color selective to both cardinal and intermediate color directions.

Cardinal and Kiper (2003) studied the global processing in chromatic Glass patterns. Half dipoles contributed to a concentric Glass pattern, referred to as signal dipoles, while the other half were randomly oriented, referred to as noise dipoles. They fixed the chromaticity of the signal dipoles and varied that of the noise dipoles. They varied the proportion of signal dipoles that coherently contributed to the concentric pattern and measured the coherence threshold of detecting a concentric pattern, and



found that the detectability varied sinusoidally as a function of noise chromaticity, regardless of signal color directions. Specifically, the coherence threshold was highest when the signal dipoles were defined in the same color direction as the noise dipoles, and lowest when the signal and noise dipoles were in opposite color directions. This finding suggested that color processing at the global stage was also color selective to both cardinal and intermediate color directions.

Similar research was done by Wilson and Switkes (2005) in which one dot chromaticity was fixed, and varied the other within dipoles, referred to as the intra-dipole condition. Or, they fixed the chromaticity of half of the dipoles and varied the other half, referred to as the inter-dipole condition. They measured the proportion of coherent dipoles needed to detect a concentric or translational Glass pattern. In the intra-dipole condition, detectability decreased as the chromaticity difference between the two dots within the dipoles increased for both concentric and translational patterns, suggesting a color-selective process at the local stage of perceptual grouping. In the inter-dipole condition, however, detectability did not change with chromaticity, suggesting a chromaticity-insensitive process at the global stage of perceptual grouping. Together, these studies (Gegenfurtner & Kiper, 2003; Mandelli & Kiper, 2005; Wilson & Switkes, 2005) revealed the color tuning properties in perceptual grouping. However, dipole Glass patterns had only one way of grouping and could not reveal complex interactions when there were multiple ways of grouping in the image. In this case, the perceptual grouping process might involve not only signal integration, but also inhibition between different ways of grouping.

To study the interaction between different ways of grouping, we used tripole Glass patterns as the stimuli. Instead of two dots, a tripole Glass pattern contained multiple sets of three dots, or tripoles (Figure 2a). One dot, called the anchor dot, determined the

random position of each tripole. The positions of the other two dots, or context dots, within a tripole were determined relatively to the position of the anchor dot (Figure 2b; see Method for details). The observers might perceive different global patterns, in a clockwise or counterclockwise spiral, if they can match the anchor dot with one or the other context dot. With tripole Glass patterns, we were able to investigate how multiple ways of grouping interacted with each other.

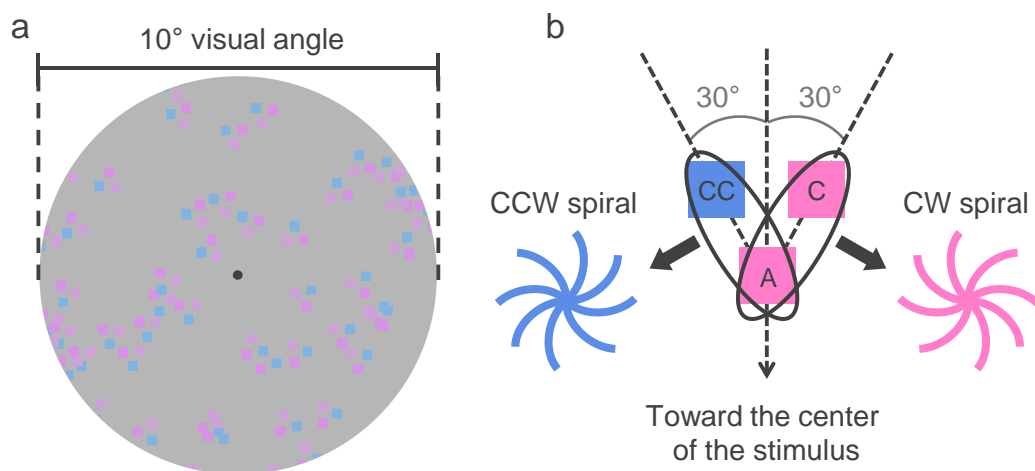


*Figure 2.* A tripole Glass pattern and the geometric description of the dots within a tripole. **a.** An example of a tripole Glass pattern. **b.** An illustration of a local tripole. A tripole consists of three dots, with one anchor dot (“A”) and two context dots (“C” and “CC”). If the visual system organizes the anchor dot with one of the context dots and integrates the resulting dot pairs over space, the observer might perceive a clockwise (CW) or counterclockwise (CCW) spiral pattern.

Tripole Glass patterns have been used to investigate contrast effects on perceptual grouping. Lin et al. (2017) used achromatic tripole Glass patterns and manipulated the luminance contrast. They found that the probability of grouping the anchor dot with one of the context dots increased as an inverted-U function as the context dot contrast

increased. Such a function shifted in a downward right direction, while the other context dot contrast increased.

Lin (2016) fixed stimulus chromaticity at one cardinal equiluminant color direction at a time and manipulated the dot color contrast in tripole Glass patterns. The probability of grouping the anchor dot with one of the context dots increased as an inverted-U or a sigmoid function, depending on the contrast range, as that context dot contrast increased. The probability function shifted in a downward right direction as the other context dot contrast increased. However, the tripole Glass patterns used in both experiments were always defined in the same achromatic or chromatic directions. The effect of chromaticity on perceptual grouping was not tested.

In the current study, we examine how chromaticity influences the perceptual grouping process and the color tuning mechanisms that support such a process. Although previous studies have investigated color tuning with concentric or translational Glass patterns embedded in randomly oriented dipoles (Mandelli & Kiper, 2005; Wilson & Switkes, 2005), we used a different approach, in which there were two possible global patterns, rather than one in the same display. Determining which global pattern would be perceived by an observer depended on how the image elements were grouped (Figure 2). That is, there were two possible ways of grouping competing with each other. Such an approach has been used to study the contrast effect of the competing global structures for luminance-defined (Lin et al., 2017) and cardinal equiluminance (Lin, 2016) patterns, but not for the competing structures with different chromaticities.

Besides dot contrast, we manipulated dot chromaticity in tripole Glass patterns. One context dot would have the same chromaticity as the anchor dot but differ only in contrast, called the same color dot or “S” dot, while the other context dot might vary both in chromaticity and contrast, called the different color dot or “D” dot (Figure 3c).

We measured the probability of grouping the anchor dot with “S” dot and saw how this probability was affected by the other pattern composed of the anchor dot and “D” dot.

We proposed two hypotheses assuming different color mechanisms: the “cardinal mechanisms hypothesis” and the “intermediate mechanisms hypothesis”.

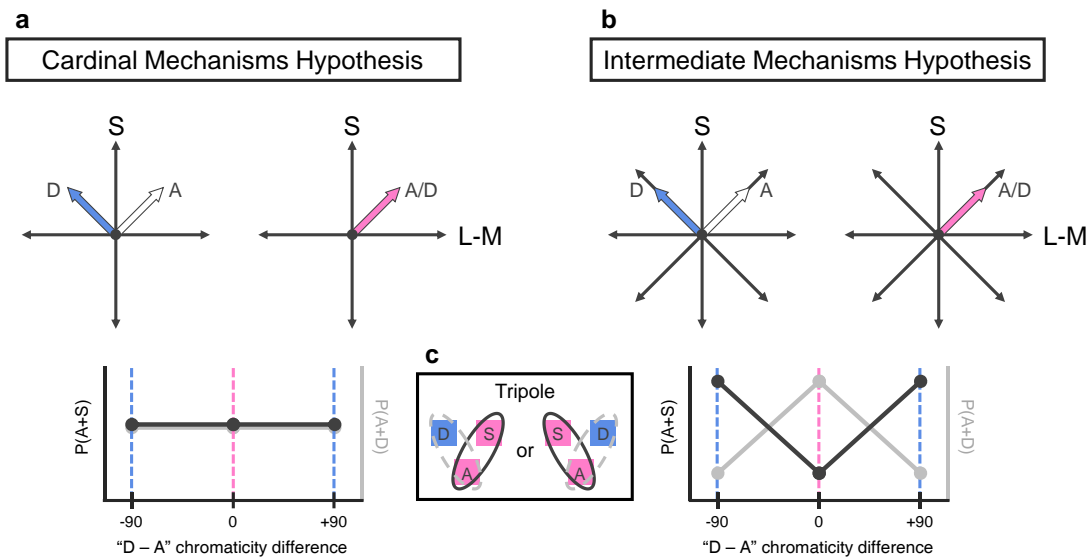


*Figure 3.* Two hypotheses for the underlying color mechanisms. The central rows of **a** and **b** illustrate the mechanism and dot color directions. The thin black arrows are the preferred color directions of the color mechanisms. The thick blue, white, and pink arrows are the dot color directions. The bottom rows are the predictions from the hypotheses. The abscissa is the chromaticity difference between the anchor dot and the different color dot. The ordinate on the left is the probability of grouping the anchor dot with the same color dot,  $P(A+S)$ . The ordinate on the right side is the probability of grouping the anchor dot with the different color dot,  $P(A+D)$ . The blue and pink dashed lines mark the conditions illustrated in the central rows. **a.** Cardinal mechanisms hypothesis: perceptual grouping is supported by cardinal color mechanisms alone. **b.** Intermediate mechanisms hypothesis: perceptual grouping is supported by additional mechanisms that prefer some intermediate colors. **c.** Illustration of the tripole. One context dot (either the clockwise or counterclockwise dot; denoted as “S”) would have the same chromaticity as the anchor dot (“A”) while the other context dot (“D”) varied in chromaticity.

In the cardinal mechanisms hypothesis (Figure 3a), perceptual grouping is supported by only cardinal mechanisms (represented by the black arrows in the central row of Figure 3a). If the anchor dot, denoted as “A”, and “D” dots are defined in different colors, and each color is intermediate to the red-green and blue-yellow cardinal colors (the thick blue and white arrows), both “A” and “D” dots would activate red-green and blue-yellow mechanisms. Perceptual grouping of “A” and “D” dots could be achieved by the signals within one of these cardinal equiluminance mechanisms.

On the other hand, when “A” and “D” dots have the same intermediate color (the pink arrow), the two dots also activate both cardinal equiluminance mechanisms and can be grouped by these mechanisms. Therefore, the probability of grouping “A” dot with “D” dot,  $P(A+D)$ , when the two dots are in different intermediate colors should be similar to the  $P(A+D)$  when the two dots are in the same intermediate color (illustrated as the gray line at the bottom of Figure 3a).

In a two-alternative forced-choice paradigm in which the observer reports perceiving global patterns composed of “A” dot and either “D” dot or “S” dot,  $P(A+D)$  is observed when “A” and “D” dots are either in the same or different intermediate colors. This is equivalent to observing the similar probability of grouping “A” dot with “S” dot, or  $P(A+S)$ , in these two conditions (the black line at the bottom of Figure 3a). The cardinal mechanisms hypothesis, therefore, would predict no intermediate color selectivity.

In the intermediate mechanisms hypothesis (Figure 3b), perceptual grouping involves extra color mechanisms that prefer some intermediate colors (represented by the black arrows in the center of Figure 3b), named as intermediate mechanisms. When “A” and “D” dots are of different intermediate colors, each dot mainly activates one of those intermediate mechanisms. Each intermediate mechanism would have a signal

from only one dot. In this case, perceptual grouping of “A” and “D” dots should be harder than the grouping in which the two dots are in the same intermediate color. Therefore,  $P(A+D)$  should be lower when the two dots are of different intermediate colors than the  $P(A+D)$  when the two dots are of the same intermediate color (the gray line at the bottom of Figure 3b). Equivalently,  $P(A+S)$  is higher when “A” and “D” dots are of different intermediate colors than the  $P(A+S)$  when “A” and “D” dots are of the same intermediate color (the black line at the bottom of Figure 3b). The intermediate mechanisms hypothesis would predict color selectivity to intermediate colors.

In addition to intuitively inferring the underlying color mechanisms from the data, we estimate color tuning functions of the mechanisms in the perceptual grouping process with a color-spatial vision model extended from that for local pattern detection (Chen et al., 2000a, 2000b) and perceptual grouping (Lin, 2016; Lin et al., 2017). With this model, we offer an integrated point of view of color processing in perceptual grouping.

## 2. Method



### 2.1. Participants

Three observers were recruited for this study. All observers had normal or corrected-to-normal visual acuity (20/20) and had no color deficits according to the Ishihara plate. One observer (LL) was the author and the others (CPY and LYS) were naïve to the purpose of the study before they completed the experiment. The observer LL attended to all experimental sessions. Each of the other two observers participated in half sessions and, together, these sessions contained all the conditions.

### 2.2. Apparatus

We presented stimuli on a 24-inch EIZO LCD (FlexScan SX2462W) monitor with  $1920 \times 1200$  resolution and 60 Hz refresh rate. The monitor was calibrated with a PR655 spectroradiometer. The background of the display during the experiment had luminance  $30.83 \text{ cd/m}^2$  and chromaticity 0.3369 and 0.3223 in CIE xy coordinates. The viewing distance was 92.7 cm. At this distance, 1 pixel corresponded to 1 arc min ( $'$ ) visual angle. The experimental control software was written in MATLAB R2010a with Psychtoolbox-3 (Brainard, 1997; Kleiner, Brainard, & Pelli, 2007; Pelli, 1997). The experiment was run in a dark room.

### 2.3. Stimulus

We used tripole Glass patterns as the stimuli. A tripole Glass pattern consisted of multiple sets of tripoles (Figure 2). Each tripole contained three dots. The positional seeds, or anchor dots, were randomly distributed across the image. The other two dots in the tripole were the context dots. Two values, radius ( $r$ ) and polar angle ( $\theta$ ), related to the anchor dot determined the positions of the context dots. The former specified the center-to-center distance between the anchor dot and each context dot while the latter determined the angle between the virtual line that connected the anchor dot and a

context dot, and the imagery radial line that linked an anchor dot to the center of the display. The radius was 17'. The polar angle was  $\pm 30^\circ$  for each context dot (Figure 2b). The size of the anchor dot and the context dots were  $7' \times 7'$ . All the dots were presented within a  $10^\circ$  diameter circular window. The total dot areas covered 4% area of the image.

If the visual system organized the anchor dot with one of the context dots, the observer would have either a clockwise or counterclockwise spiral percept (Figure 2b). Hence, we named the context dots potentially leading to either a clockwise or a counterclockwise spiral as the clockwise (CW) and counterclockwise (CCW) dots, respectively.

The color of the tripole Glass patterns was defined in a MBDKL color space (Derrington et al., 1984; Krauskopf, Williams, & Heeley, 1982; MacLeod & Boynton, 1979). The three axes of the space were the achromatic (L+M+S), red-green (L-M), and blue-yellow (S) axes. These were the linear combinations of the L, M, and S cone signals, in which each axis independently activated one cardinal mechanism (luminance (L+M), red-green (L-M), or blue-yellow (S-[L+M]) mechanisms). Cone excitations were calculated by multiplying the measured spectral power distributions with the 10-degree cone fundamentals estimated by Stockman and Sharpe (2000). The origin of the color space was at the background chromaticity, or cone excitation,  $[L_{BG}, M_{BG}, S_{BG}] = [2.426, 2.085, 1.224]$ .

In this study, we used colors on the nominal equiluminant plane spanned by L-M and S axes. We measured the contrast detection threshold at several color directions for each observer (see Appendix A for threshold measurement details). These thresholds were fitted with an ellipse. The aspect ratio of the ellipse was used to normalize the two cardinal equiluminant axes. Colors used in the experiment were chosen from the



normalized color space. Since the detection thresholds, and the aspect ratio of the fitted ellipse, varied among observers, such normalization was observer dependent. However, the inter-observer variability was small.

Color on the equiluminant plane could be described either by their L-, M-, S-cone contrast modulations, or by polar coordinates with color contrast ( $C$ ) and azimuth ( $\phi$ ) (Figure 4). Color contrast ( $C$ ) corresponded to the distance from the adapting point to the end of the color vector, and was defined as the squared root of the averaged cone contrast energies (Brainard, 1996). That is,

$$C = \sqrt{(C_L^2 + C_M^2 + C_S^2)/3}$$

where L-cone contrast,  $C_L$ , was the stimulus L-cone excitation,  $L$ , deviated from the background excitation,  $L_{BG}$ , and divided by the L-cone excitation of the background:

$$C_L = \frac{L - L_{BG}}{L_{BG}}$$

M-cone contrast,  $C_M$ , and S-cone contrast,  $C_S$ , were defined similarly.

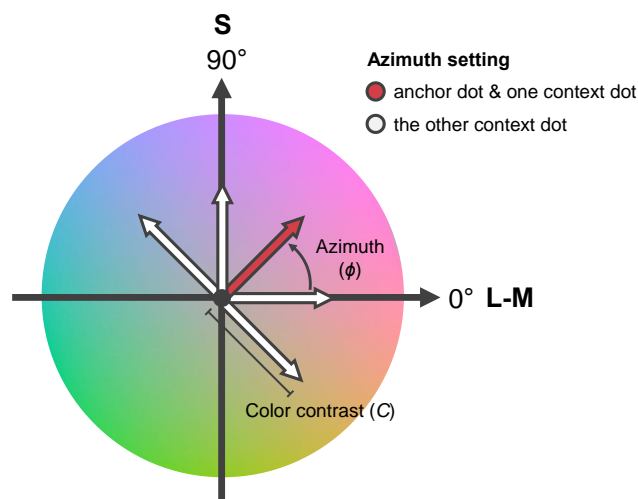
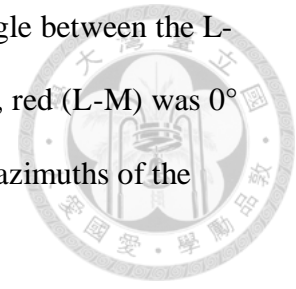


Figure 4. The equiluminant plane. Azimuth ( $\phi$ ) is the polar angle from L-M axis to the direction of the color vector. Color contrast ( $C$ ) is the length of the vector, or the distance from the origin to the end of the vector. Some color vectors used in the experiment were also illustrated (see stimulus settings for details).

The azimuth ( $\phi$ ), corresponding to the chromaticity, was the angle between the L-M axis and the color direction of that stimulus. In our representation, red (L-M) was  $0^\circ$  and blue (S) was  $90^\circ$ . The normalized cone contrast vectors and the azimuths of the stimuli are listed in Table A1 in Appendix A.



The anchor dot chromaticity was set at four cardinal directions ( $0^\circ$ ,  $90^\circ$ ,  $180^\circ$ , or  $270^\circ$ ) or four intermediate directions ( $45^\circ$ ,  $135^\circ$ ,  $225^\circ$ , or  $315^\circ$ ). One context dot chromaticity would be the same as the anchor dot, while the other was chosen within the range of  $\pm 90^\circ$  at  $45^\circ$  intervals relative to the anchor dot chromaticity. The context dot paired with the same chromaticity as the anchor dot could be a CW or CCW dot.

Color contrast was defined in multiples of the detection threshold. Anchor dot contrast was fixed at twice the detection threshold of a given chromaticity. Each context dot contrast varied independently from approximately 1- to 4-fold the detection threshold of the corresponding chromaticity. Figure 5 shows some stimulus examples.

## 2.4. Procedure

We used a two-alternative forced-choice (2AFC) paradigm. The observers participated in four (CPY and LYS) or eight (LL) experimental sessions. Each session contained one anchor dot chromaticity paired with five context dot chromaticities. Different chromaticity combinations were separated in different runs and each combination repeated ten runs. Within each run, five contrasts to each context dot were shown in randomized order. Each contrast combination was repeated four times.

Each trial began with a beeper. A fixation point was presented for 800 ms and remained visible during the stimulus presentation. A Glass pattern was shown for 500 ms. Observers reported the pattern orientation, either clockwise or counterclockwise, by pressing the buttons on the keyboard, and a feedback sound was provided. The next trial began after the response.

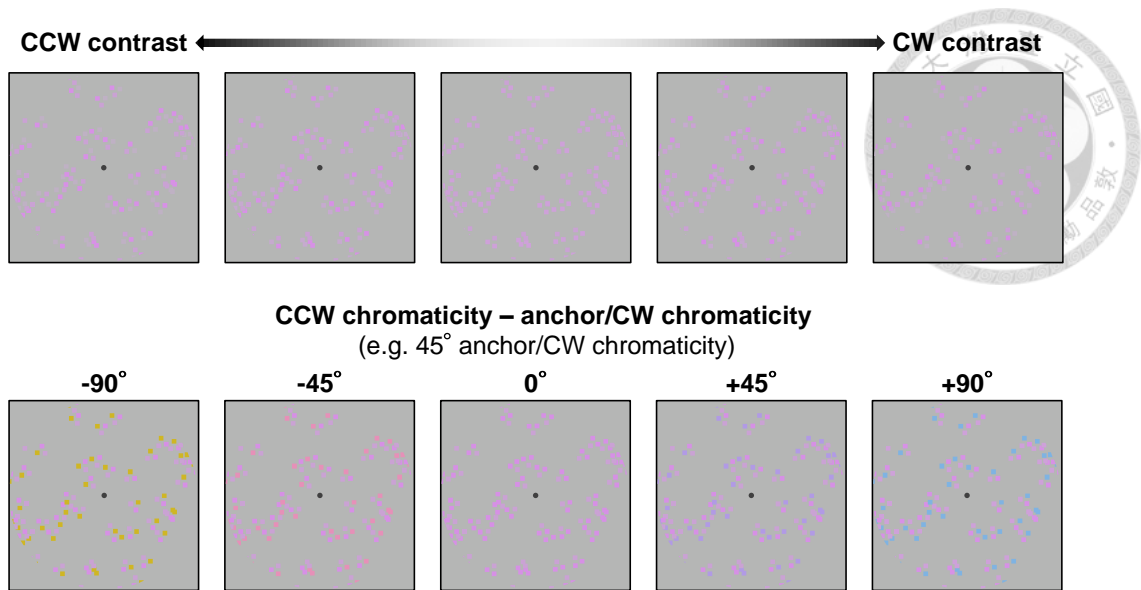
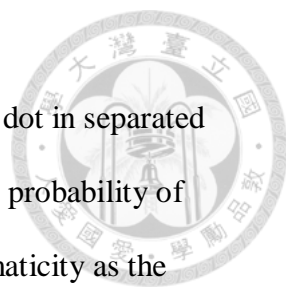


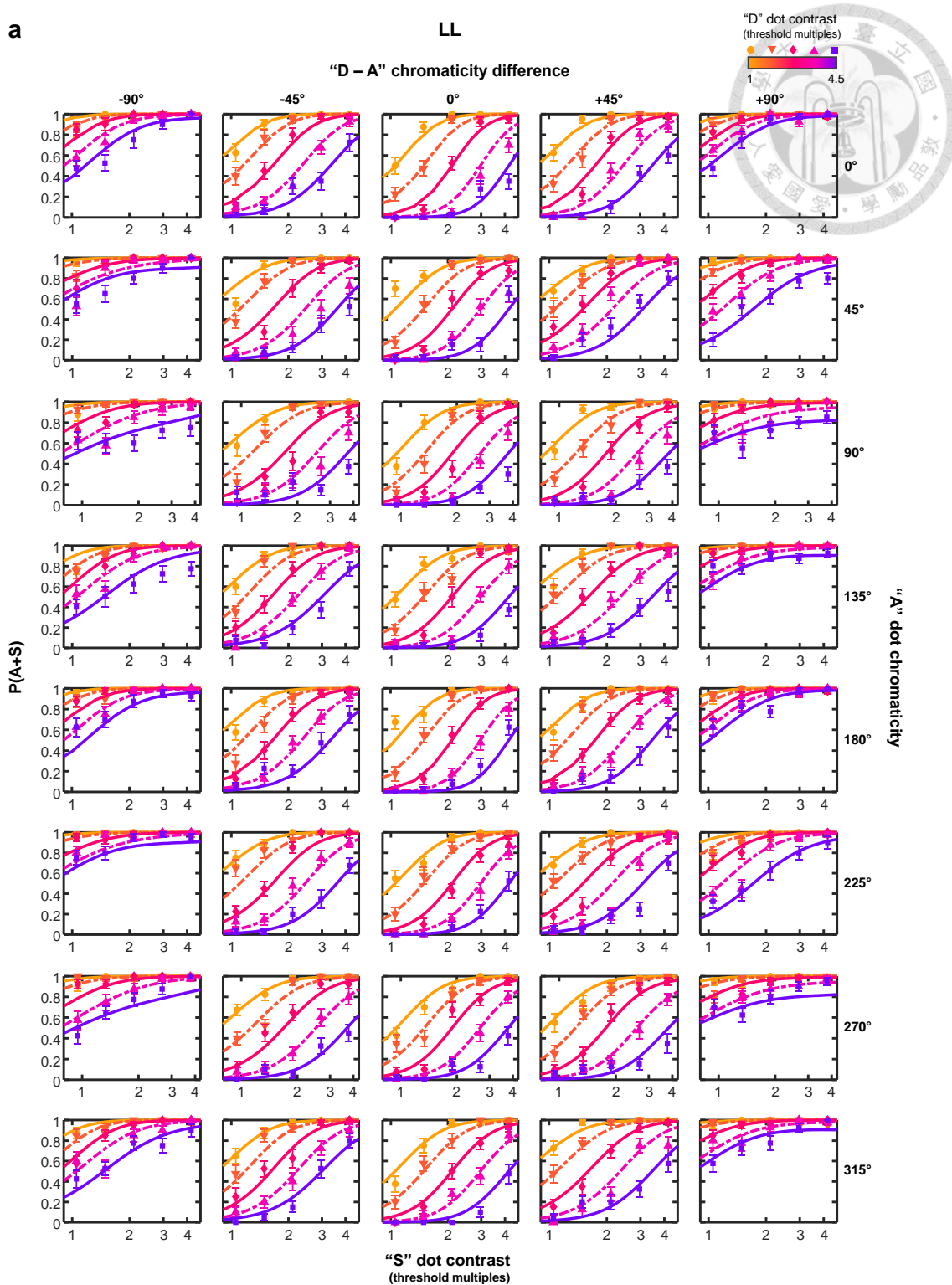
Figure 5. Examples of the tripole Glass patterns. *Upper row*: context dot contrast variations. The clockwise (CW) dot contrast increases from the leftmost image to the rightmost image. The counterclockwise (CCW) dot contrast increases in the opposite direction. *Lower row*: CCW dot chromaticity variation. In these examples, CCW dot chromaticity differs from 45° anchor/CW dot chromaticity from -90° to +90°. The color vectors of the examples on the equiluminant plane are illustrated in Figure 4.

### 3. Result



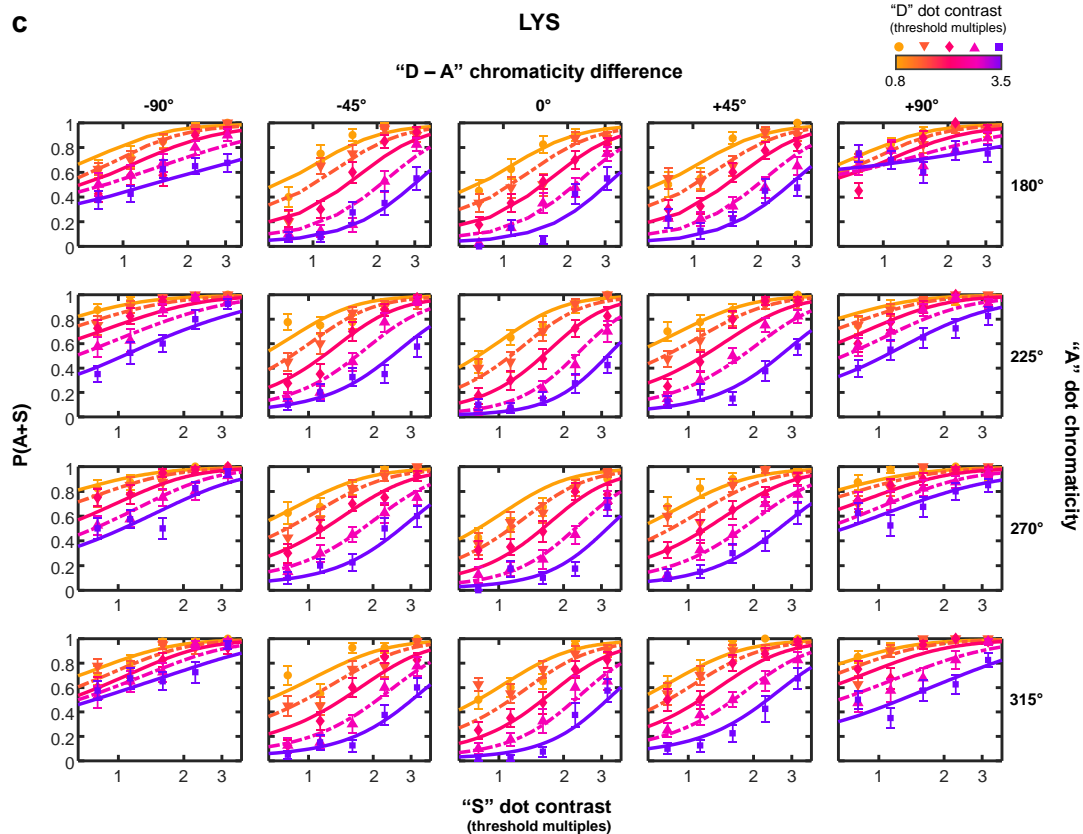
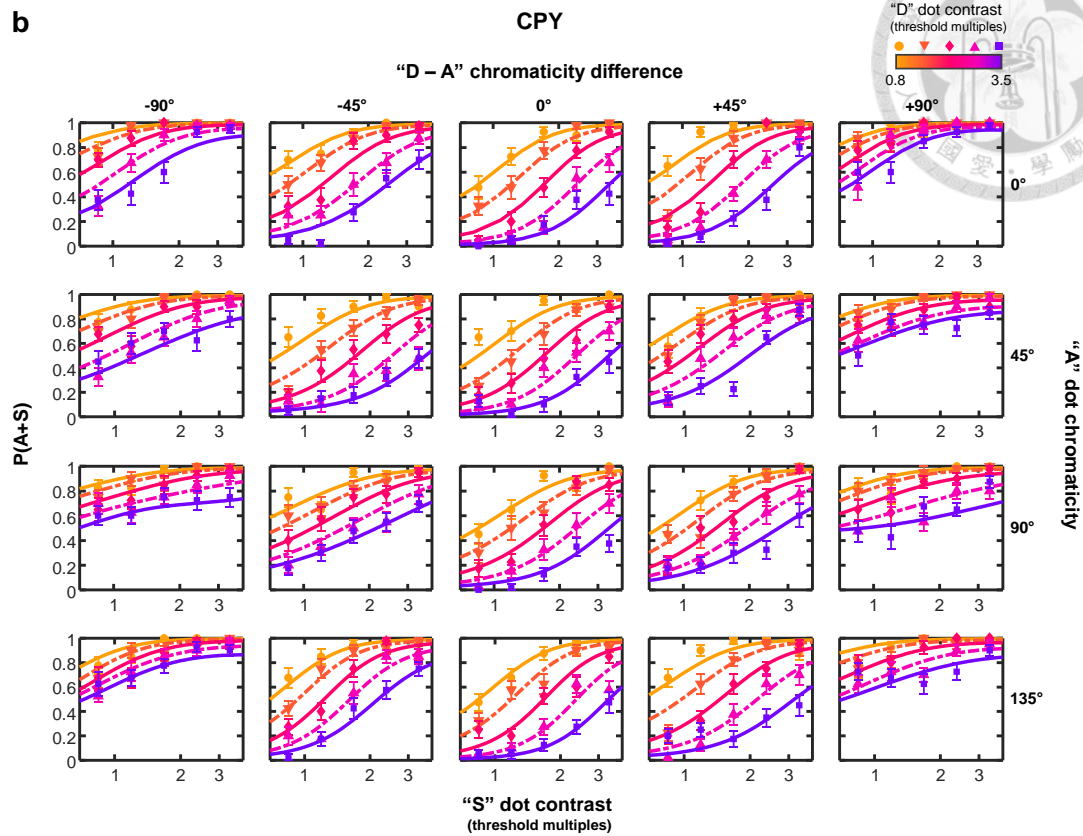
The CW and CCW dot had the same chromaticity as the anchor dot in separated half trials (illustrated in Figure 3c). We first separately calculated the probability of grouping the anchor dot with the context dot that had the same chromaticity as the anchor dot in these two sets of trials. The probability distributions of these two sets of data were the same for LL ( $\chi^2(999, N = 20) = 165.88, p > .9999$ ), CPY ( $\chi^2(499, N = 20) = 193.64, p > .9999$ ), and LYS ( $\chi^2(499, N = 20) = 131.95, p > .9999$ ), indicating that the observers were not biased toward any global pattern orientation (CW or CCW spiral) by the pairing of dot position and chromaticity. Therefore, we averaged the probability of grouping the anchor dot with the same color dot of these two sets of data. To simplify the discussion, the context dot having the same chromaticity as the anchor dot was named the same color dot, or “S” dot. The context dot varying in chromaticity was named the different color dot, or “D” dot. We presented the probability of grouping the anchor dot (denoted as “A”) with “S” dot under different dot contrast and chromaticity combinations. The position naming for the context dots, CW or CCW dot, was used only when mentioning dot position was necessary. Otherwise, we used color naming, “D” or “S” dot, in the following text.

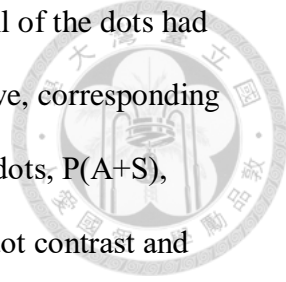
Figure 6a-c shows the performance of the three observers. Each row represents one anchor (“A”) dot chromaticity, labelled on the right side. Each column shows the different color (“D”) dot to “A” dot chromaticity difference. The abscissa represents the same color (“S”) dot contrast. The ordinate is the probability of grouping “A” and “S” dots, or  $P(A+S)$ . Different colored symbols are for different “D” dot contrasts. The legend for these symbols can be found in the upper right position of the figure. The smooth lines are the fitting curves.



*Figure 6.* The probability of grouping the anchor dot and the same color dot under different contrast and chromaticity combinations. Each row shows one anchor (“A”) dot chromaticity. Each column shows the chromaticity difference between “A” dot and the different color (“D”) dot. The abscissa is the same color (“S”) dot contrast. The ordinate is the probability of grouping “A” and “S” dots. Different symbols and lines correspond to “D” dot contrast levels and the model fits. **a.** The observer LL. **b.** CPY. **c.** LYS. (Continued.)

Figure 6. (Continued.)

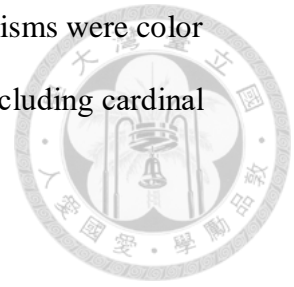




For the contrast effect, we first described the conditions when all of the dots had the same chromaticity (the central plot in each row). For a single curve, corresponding to a fixed “D” dot contrast, the probability of grouping “A” and “S” dots,  $P(A+S)$ , increased with “S” dot contrast.  $P(A+S)$  increased faster at low “S” dot contrast and slower at high contrast, showing a sigmoid shape function. In our manipulated contrast range, this trend was especially clear for the red colored curve. On the other hand, given a fixed “S” dot contrast,  $P(A+S)$  decreased as the “D” dot contrast increased, causing the probability function to shift in a downward right direction. This could be seen by comparing the low “D” dot contrast curve (e.g., the orange curve) with the high “D” dot contrast curve (e.g., the purple curve). Since the probabilities of grouping “A” dot with either “D” dot or “S” dot summed to unity, the decreased  $P(A+S)$  was equivalent to the increased probability of grouping “A” and “D” dots, suggesting that the observers perceived more often the spiral patterns composed of “A” and “D” dots as “D” dot contrast increased. This indicated that the two ways of grouping, “A” with either “D” or “S”, increased with their dot contrasts, respectively, suggesting that the two ways of grouping competed with each other for the percept.

For the chromaticity effect, we compared  $P(A+S)$  for different “D” to “A” chromaticity difference conditions (shown by the plots in each row). From the outer plots to the central plot in a given row of Figure 6a-c ( $\pm 90^\circ$  toward  $0^\circ$  “D” to “A” chromaticity difference), the same colored curve (e.g., the purple curve) moved downward as the “D” to “A” chromaticity difference decreased. In other words,  $P(A+S)$  decreased when the “D” to “A” chromaticity difference decreased. This was the same thing as saying that the probability of grouping “A” dot with “D” dot increased as the chromaticity difference between “A” and “D” dots decreased, suggesting that perceptual grouping of “A” dot with “D” dot was improved as the chromaticity difference between

these two dots became smaller, and that perceptual grouping mechanisms were color selective. We observed these trends for all “A” dot chromaticities, including cardinal and intermediate chromaticities.





## 4. Discussion



In the current study, we investigated color mechanisms in perceptual grouping by manipulating chromaticity as well as contrast of the image elements in tripole Glass patterns.

### 4.1. The contrast effect on perceptual grouping

We found that perceptual grouping of one global pattern with other simultaneously presented patterns is influenced by both the dot contrast of that global pattern and the other pattern. The probability of perceiving one global pattern increased as a sigmoid function as the dot contrast of that pattern increased. The probability function shifted in a downward right direction as the dot contrast of the other pattern increased. This finding replicated the result done by Lin (2016). Lin (2016) manipulated dot color contrast in tripole Glass patterns defined on cardinal equiluminant axes. At the contrast range similar to our study, the probability of grouping the anchor dot with one context dot increased monotonically with the context dot contrast. Such a probability function shifted to downward right as the other context dot contrast increased. At higher context dot contrast and lower anchor dot contrast for red and green stimuli, they found that the probability increased to a critical point and then decreased, showing an inverted-U shape function. In our study, we used equally perceivable contrasts for different color directions. Due to the limited producible contrast in the blue-yellow color direction, we were not able to include even higher contrast for other color directions. Therefore, we did not get the inverted-U shape function in our result.

### 4.2. The role of gain control

Previous studies have indicated that cortical neurons adjust their responses not only with contrast of their preferred pattern, but also with contrast of the other patterns (Carandini, Heeger, & Movshon, 1997; Freeman, Durand, Kiper, & Carandini, 2002;

Geisler & Albrecht, 1992). Such a property is called contrast gain control, which allows the neurons to respond within a suitable range under different contexts. The contrast gain of the cortical neuron increases at low stimulus contrast and decreases at high contrast, resulting in a sigmoidal contrast response function. Contrast gain decreases when another stimuli is simultaneously presented (Carandini et al., 1997; Freeman et al., 2002; Geisler & Albrecht, 1992), or when the subject adapts to a higher contrast stimulus (Ohzawa, Sclar, & Freeman, 1982, 1985), making the contrast function shift in a downward right direction.

Psychophysical pattern vision models introduced the concept of gain control through divisive inhibition (Chen et al., 2000b; Foley, 1994; Huang & Chen, 2016; Lin et al., 2017; Teo & Heeger, 1994; Watson & Solomon, 1997). For example, Foley (1994) proposed that the response of a global pattern detector,  $R$ , was the detector excitation,  $E$ , raised to an exponent,  $p$ , and divided by the inhibitions from all detectors,  $I$ , plus an inhibitory constant,  $z$ .

$$R = \frac{E^p}{I + z}$$

In our case, for example, when the contrast of the context dot at the clockwise (CW) position increased, the excitation of the global pattern detector that preferred the grouping of the anchor dot and CW context dot would increase. Also, such a pattern detector, or CW pattern detector, received more inhibition from the detector itself as the CW dot contrast increased. At low CW dot contrast, the inhibition to the CW pattern detector was relatively small compared to the inhibitory constant. Therefore, the CW detector response exponentially increased with the excitation as contrast increased. However, at high CW contrast, the inhibition from the CW pattern detector itself exceeded that of the constant, decelerating the detector response when CW contrast further increased, and resulted in the S-shape contrast function.

On the other hand, the inhibition from the counterclockwise (CCW) pattern detector to the CW pattern detector increased when the CCW dot contrast increased. Thus, the CW detector response decreased as the CCW dot contrast increased, shifting the response function in a downward right direction.

Such a model, called the divisive inhibition model, has successfully explained perceptual grouping in tripole Glass patterns modulated in luminance contrast (Lin et al., 2017), and cardinal equiluminance color contrast (Lin, 2016), suggesting that a similar model structure could be applied to our data as well. However, the models were built to account for stimuli modulated on a single axis in a color space. Our stimuli contained dots modulated on multiple axes, or in different chromaticities. We needed to modify the model to account for the chromaticity effect on perceptual grouping.

#### **4.3. The chromaticity effect on perceptual grouping**

We manipulated the chromaticity of the dots in tripole Glass patterns. One context dot chromaticity could deviate from that of the other two dots. Therefore, we were able to measure the influence of the different color (“D”) dot on the grouping of the anchor (“A”) dot and the same color (“S”) dot. We observed that the probability of grouping “A” dot with “S” dot decreased when the “D” to “A” chromaticity difference decreased. Since the probability of grouping “A” dot with either “S” or “D” dot summed to unity, the probability of grouping “A” dot with “D” dot increased when the chromaticity difference between the “A” and “D” dots decreased. This indicated that the perceptual grouping process was color selective. Importantly, we found color selectivity in both cardinal and intermediate color directions.

As mentioned in the Introduction and Figure 3, the cardinal mechanisms hypothesis describes how the perceptual grouping process is supported by cardinal mechanisms alone. Since “A” and “D” dots defined in different intermediate color

directions activate both cardinal equiluminance mechanisms, the visual system could integrate these two dots by the signals within these mechanisms. Thus, the probability of grouping the two dots should remain relatively unchanged when the two dots are in different intermediate colors compared to the probability when they are in the same intermediate color. The cardinal mechanisms hypothesis predicted no intermediate color selectivity.

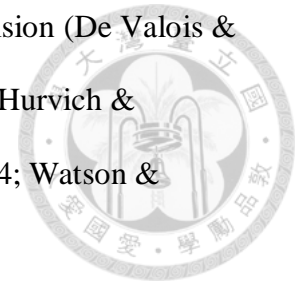
In contrast, the intermediate mechanisms hypothesis assumed that additional color mechanisms that preferred intermediate colors were involved in the perceptual grouping process. “A” and “D” dots in different intermediate colors would activate different intermediate mechanisms, and each intermediate mechanism received a signal from only one dot. The visual system could not use the signal within each mechanism to organize the two dots, therefore, the probability of grouping the two dots in different intermediate colors should be lower than the probability of grouping the two dots in the same intermediate color. The intermediate mechanisms hypothesis predicted color selectivity to intermediate colors. Our result was consistent with the prediction of the intermediate mechanisms hypothesis, suggesting that the perceptual grouping process involves extra color mechanisms than the cardinal mechanisms.

#### **4.4. Modeling chromatic mechanisms**

In addition to intuitively inferring the underlying color mechanisms from the data, we could estimate the mechanisms through a modelling approach.

Previously, Chen et al. (2000b) modelled color mechanisms in a simple pattern detection in a masking paradigm. They measured the detection threshold of a Gabor patch against the contrast of another superimposed Gabor, called a pedestal. The target and the pedestal could modulate on either the same or different color axes. Generally, the detection threshold decreased first and then increased as the pedestal contrast

increased. The model included the main characteristics from color vision (De Valois & De Valois, 1993; Guth, 1991; Guth, Massof, & Benzschawel, 1980; Hurvich & Jameson, 1957) and pattern vision (Foley, 1994; Teo & Heeger, 1994; Watson & Solomon, 1997).



At the initial stage, the model had color-spatial detectors that defined the receptive field of the color mechanisms. These mechanisms linearly combined cone signals. The excitation to the stimulus was calculated for each color mechanism. At the latter stage, like most pattern vision models (Chen et al., 2000b; Foley, 1994; Huang & Chen, 2016; Lin, 2016; Lin et al., 2017; Teo & Heeger, 1994; Watson & Solomon, 1997), the mechanism excitation went through a nonlinear operation, or a divisive inhibition process more specifically, to determine the mechanism response. Finally, the responses of all color mechanisms were combined to determine the pattern detection performance. In this model, the contrast gains with respect to the LMS cones determined the preferred color direction of the mechanism. Chen et al. (2000b) was able to estimate the contrast gains for each color mechanism with no assumption on the shape of the mechanism tuning function.

We followed the approach of Chen et al. (2000b) and implemented different numbers of color mechanisms into our model. Except for the general model structure, our model differs from theirs in some ways. First, their model was designed for Gabor pattern detection, whereas ours was for perceptual grouping in tripole Glass patterns. Chen et al. (2000b) fixed the orientation of the Gabor patch. Therefore, they could assume that all the detectors had the orientation preference corresponding to the Gabor orientation. Tripole Glass patterns contain randomly distributed tripoles in the image, and the orientation of the line connecting any two dots in a tripole depends on the absolute location of that tripole. If the detector has the orientation preference parallel to

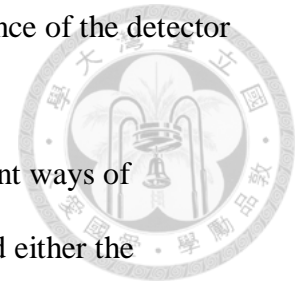
the line connecting two dots in a tripole, then the orientation preference of the detector also depends on the location of the tripole.

The orientation preference of the detector also differs in different ways of grouping. For example, the dot pairs consisting of the anchor dot and either the clockwise or counterclockwise dot would activate different orientation detectors. For these reasons, we assumed that the local detectors in our model had several orientation preferences.

Second, with the detector optimally activated by the Gabor patch, the detector excitation was proportional to the linear sum of cone signals at the center location of the Gabor patch. Our stimuli were dots separated in space. Two dots covered by the receptive field of a local detector were modulated independently in chromaticity. Thus, the detector excitation was determined by the sum activations of these two dots.

Third, in contrast to simple pattern detection that required only the local detectors, our model has a global stage that contains global pattern detector receiving signals from the local detectors. Previous studies have suggested that the global detector linearly summed the signals from the local detectors (Wilson et al., 1997), and the nonlinear relationship between the global detector output and the mechanism response occurred afterward.

In sum, we extended the models from that used in explaining the detection of Gabor patterns (Chen et al., 2000a, 2000b) and those in perceptual grouping with luminance-defined (Lin et al., 2017), or single-colored (Lin, 2016), stimuli. We tested models with different numbers of color mechanisms and estimated the sensitivity functions of these mechanisms in order to build an understanding of the underlying color mechanisms in perceptual grouping and the color-tuning properties of those mechanisms.



#### 4.5. Model overview

Figure 7 shows the model diagram. In the following description of the model, we refer to the context dots as the clockwise (CW) and counterclockwise (CCW) dots instead of same and different color dots. This naming corresponds to the task for the observer (they were asked to report the pattern orientation of the Glass patterns). To link to the color name, same or different color dot, the CW dot is illustrated as the same color dot while the CCW dot is the different color dot.

The perceptual grouping process starts with local tripoles in the image. At the first stage, there are local color-spatial linear operators extracting color and orientation information from the dipoles in tripoles. At the second stage, operator excitations are summed together and sent to the global pattern detector. The excitation of the pattern detector is half-wave rectified, and the response of the detector is determined by the divisive inhibition process. Next, chromatic mechanism responses are combined by the preferred pattern orientation of the detectors. Finally, the decision value is the difference between CW and CCW pattern responses. Below, we provide a quantitative description of the model.

#### 4.6. The quantitative description of the model

Table A2 in Appendix B summarizes the symbols used in the following text.

The inputs of the model were cone contrast vectors. In this case, the only assumption on chromatic detection is that the mechanisms linearly combine cone signals (Sankeralli & Mullen, 2001).

The local operator defines the receptive field of the chromatic mechanism. Assume that the preferred orientations of the operators are paralleled to the lines connecting any two dots (anchor and CW, anchor and CCW, or CW and CCW) within a tripole, and that the center of the operator corresponds to the midpoint between the two dots.

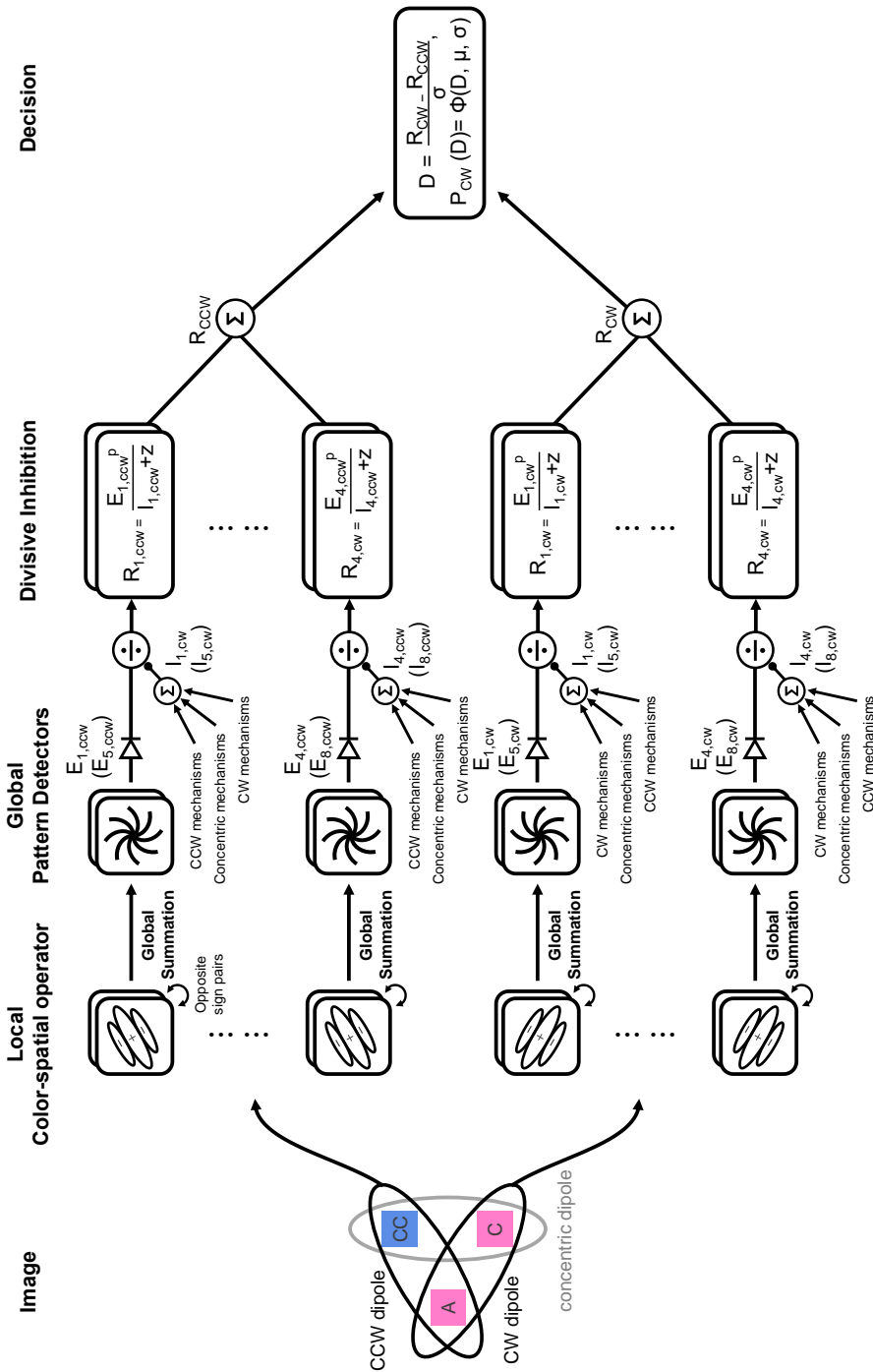


Figure 7. A schematic diagram of the divisive inhibition model. The perceptual grouping process begins with local tripoles (“A” for anchor dot, “C” for clockwise dot, and “CC” for counterclockwise dot). Any dot pair, within a tripole is processed by color-spatial linear operators. Then, the operator excitations are integrated by the global pattern detector. The response of the pattern detector is determined by the divisive inhibition process in which the excitation is raised by a power and divided by the inhibition plus a constant. The responses of the chromatic mechanisms are summed according to the preferred pattern orientation of the detectors. Finally, the decision value is the difference between CW and CCW pattern responses. The process for a task-irrelevant concentric pattern is not shown explicitly in this illustration.



According to Poirson and Wandell (1996), the spatial and chromatic properties of a mechanism are separable. Therefore, chromatic and spatial components can be separately calculated and then multiplied together. The operator excitation,  $Ed_j$ , is the inner product of dot cone contrasts and the chromatic gains summed across space:

$$Ed'_j = \mathbf{C}_1^T \mathbf{G}_j \int I_1(x, y) \times f(\Delta x, \Delta y) dx dy + \mathbf{C}_2^T \mathbf{G}_j \int I_2(x, y) \times f(\Delta x, \Delta y) dx dy \quad (1)$$

The subscript  $j = 1, 2, \dots, J$  indicates the operator with the  $j^{\text{th}}$  chromatic mechanism.  $\mathbf{C}_1$  and  $\mathbf{C}_2$  are three-element column vectors specifying the L, M, S cone contrast of the two dots. That is,  $\mathbf{C}_1 = [C_{L1}, C_{M1}, C_{S1}]^T$  and  $\mathbf{C}_2 = [C_{L2}, C_{M2}, C_{S2}]^T$ .  $\mathbf{G}_j$  is the contrast gain of the  $j^{\text{th}}$  chromatic mechanism with respect to the three cone classes, or  $\mathbf{G}_j = [G_{Lj}, G_{Mj}, G_{Sj}]^T$ . These two vectors define the chromatic contribution to the excitation.  $I_1(x, y)$  and  $I_2(x, y)$  describe the spatial modulations of the two dots.  $f(\Delta x, \Delta y)$  is the spatial description of the operator where  $\Delta x = x - x_0$ ,  $\Delta y = y - y_0$ , and  $x_0$  and  $y_0$  represent the midpoint between the two dot centers. The terms in the integral define the spatial contribution to the excitation.

Since all spatial properties of the dots except for their positions were the same in the experiment, and provided that the two dots are symmetric on the center of the operator,  $I_1(x, y)$  and  $I_2(x, y)$  can be simplified into a single term,  $I(x, y)$ . Therefore, the excitation of the operator is simplified as:

$$Ed'_j = (\mathbf{C}_1^T + \mathbf{C}_2^T) \mathbf{G}_j \int I(x, y) \times f(\Delta x, \Delta y) dx dy \quad (2)$$

The excitation of the global pattern detector is the summed activation by the constituent dipoles. Assume that there are  $n$  dipoles activating the global detector. The excitation of the global detector is:

$$E'_j = n \times Ed'_j = (\mathbf{C}_1^T + \mathbf{C}_2^T) \mathbf{S}e_j \quad (3)$$

where  $\mathbf{S}e_j$  is  $[\text{Se}_{Lj}, \text{Se}_{Mj}, \text{Se}_{Sj}]^T$  and

$$\text{Se}_{Lj} = n \times G_{Lj} \int I(x, y) \times f(\Delta x, \Delta y) dx dy \quad (4)$$



with  $\text{Se}_{Mj}$  and  $\text{Se}_{Sj}$  defined similarly.  $\mathbf{S}e_j$  is called the contrast sensitivity of the global detector with the  $j^{\text{th}}$  chromatic mechanism. Any two dots in the tripoles have a potential to be organized into a global pattern. For example, grouping the anchor dot with CW or CCW dot results in a clockwise (CW) or counterclockwise (CCW) spiral pattern, and grouping CW and CCW dots result in a task-irrelevant concentric pattern. If we have a number of  $J$  chromatic mechanisms with different color tunings, each type of pattern detector would be paired with these  $J$  chromatic mechanisms. We give a second subscript  $\rho = CW, CCW, \text{ or } concentric$  to indicate the preferred pattern orientation of these global detectors:

$$E'_{j,\rho} = n \times Ed'_{j,\rho} = (\mathbf{C}_1^T + \mathbf{C}_2^T) \mathbf{S}e_j \quad (5)$$

The excitation is then half-wave rectified so that it is never a negative value:

$$E_{j,\rho} = \max(0, E'_{j,\rho}) \quad (6)$$

Such an operation simulates the response properties of cortical cells, which have been known to have a low maintained discharge (Carandini, Heeger, & Movshon, 1999).

The response of the detector is determined by the divisive inhibition process:

$$R_{j,\rho} = \frac{E_{j,\rho}^p}{I_{j,\rho} + z} \quad (7)$$

The response of the detector with  $j^{\text{th}}$  chromatic mechanism and  $\rho$  preferred pattern orientation,  $R_{j,\rho}$ , is the excitation,  $E_{j,\rho}$ , raised by a power  $p$  and divided by the inhibition,  $I_{j,\rho}$ , plus a constant  $z$ .

The inhibition term,  $I_{j,\rho}$ , is the sum of weighted excitations of all detectors each raised by a power  $q$ :

$$I_{j,\rho} = \sum_{\rho'} \sum_i (S_{ij,\rho'} \times E_{i,\rho'})^q \quad (8)$$



The subscript  $\rho' = CW, CCW, \text{ or } concentric$  and  $i = 1, 2, \dots, J$  represent the preferred pattern orientation and the chromatic mechanism of the detector sending the inhibition.

$\rho = CW, CCW, \text{ or } concentric$  and  $j = 1, 2, \dots, J$  represent the preferred pattern orientation and the chromatic mechanism of the detector receiving the inhibition.  $S_{ij,\rho'}$  is the inhibitory weight for the inhibitory signal from the detector with the  $i^{th}$  chromatic mechanism and  $\rho'$  preferred pattern orientation to the detector with the  $j^{th}$  chromatic mechanism and  $\rho$  preferred pattern orientation.

The responses of different color mechanisms are combined by the Minkowski summation, which gives the pattern response,  $R_\rho$ :

$$R_\rho = \left( \sum_j R_{j,\rho}^m \right)^{1/m} \quad (9)$$

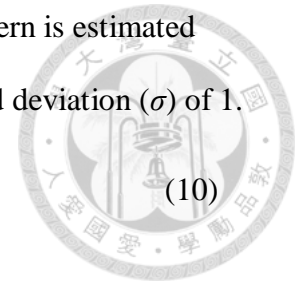
The parameter  $m$  determines the rule for combining mechanism responses. For example,  $m = 2$  represents the distance rule; a value larger than 2 corresponds to probability summation (Quick, 1974).

The concentric pattern response should be irrelevant to the decision due to our 2AFC experimental setting. Therefore, the decision variable,  $D$ , is determined only by the difference between CW and CCW pattern responses and divided by the internal noise,  $\sigma$ :

$$D = \frac{R_{CW} - R_{CCW}}{\sigma} \quad (10)$$

The probability of choosing the CW pattern over the CCW pattern is estimated from a cumulative Gaussian function with 0 mean ( $\mu$ ) and a standard deviation ( $\sigma$ ) of 1.

$$P_{CW}(D) = \Phi(D, \mu, \sigma) \quad (10)$$



#### 4.7. Model implementation and performance

We made some simplifications in implementing the model. First, the chromatic mechanisms were grouped into opposite sign pairs. Within each opposite sign pair, one mechanism sensitivity was negative to the other. For example, a model with eight chromatic mechanisms is equivalent to a model with four pairs of chromatic mechanisms. In a model with four pairs of chromatic mechanisms, the first to the fourth mechanism sensitivities ( $Se_1, Se_2, Se_3, Se_4$ ) were set to the negative of the fifth to the eighth mechanism sensitivities ( $Se_5, Se_6, Se_7, Se_8$ ). We described the tested models by the number of pairs of chromatic mechanisms instead of the number of mechanisms in the following text. For example, we described a model with eight chromatic mechanisms as a 4-pair model.

The number of inhibitory weights in the 4-pair model was 198 in general. That is, 8 (chromatic mechanisms sending inhibitions)  $\times$  8 (chromatic mechanisms receiving the inhibitions)  $\times$  3 (for CW, CCW, and concentric pattern detectors). Two constraints were made to reduce the number of these free parameters. First, the chromatic mechanisms in an opposite sign pair behaved similarly so that their inhibitions to other mechanisms, including the inhibitions to each other, were the same. Second, regarding the preferred pattern orientation, the inhibitions were roughly segregated into two parts, either those from mechanisms of the same or different preferred orientations. Inhibitory weights of these two parts were called “same orientation inhibition” ( $SiS$ ) and “different orientation inhibition” ( $SiD$ ), respectively. These constraints reduced the number of free parameters

for these inhibitory weights to 32. The inhibition could be rewritten as:  $I_{j,\rho} =$

$$\sum_i (S_i S_{ij} \times E_{i,\rho})^q + \sum_{\rho' \neq \rho} \sum_i (S_i D_{ij} \times E_{i,\rho'})^q.$$

The parameter  $m$  that determined the rule of combining mechanism responses was estimated with the Weibull psychometric function for red-green (Eskew, Stromeyer, Picotte, & Kronauer, 1991) and blue-yellow (Watanabe, Smith, & Pokorny, 1997) mechanisms, and was approximately equal to 2. Therefore, we set  $m$  to 2.

The parameters were estimated using all obtained data of an observer (1000 for LL, and 500 for CPY and LYS). The 4-pair model explained about 94 to 97% of variances. The root mean square errors (RMSEs) were about 0.06 and the mean standard errors of the data were around 0.04 to 0.05. The smooth curves in Figure 6a-c were the prediction of the best fits. The best-fitted parameters are listed in Table A3 in the Appendix C.

#### 4.8. Tests on the number of chromatic mechanisms

The simpler models with two or three pairs of mechanisms were compared with the 4-pair model. These models were equivalent to one or two fixed sets of contrast sensitivities, and the relevant inhibitory weights, to zeros. The number of free parameters decreased from 47 to 30 from a 4-pair model to a 3-pair model, and to 17 to a 2-pair model. Model comparison statistics showed that the 4-pair model was better than the 3-pair model for LL ( $F(17,952) = 15.14, p < .0001; \Delta BIC_{4pair/3pair} = -121.87, Pr_{BIC}(3pair/Data) < .0001$ ), CPY ( $F(17,452) = 6.31, p < .0001; \Delta BIC_{4pair/3pair} = -0.81, Pr_{BIC}(3pair/Data) = .401$ ), and LYS ( $F(17,452) = 6.86, p < .0001; \Delta BIC_{4pair/3pair} = -9.15, Pr_{BIC}(3pair/Data) = .010$ ) and better than the 2-pair model for LL ( $F(30,952) = 52.73, p < .0001; \Delta BIC_{4pair/2pair} = -771.74, Pr_{BIC}(2pair/Data) < .0001$ ), CPY ( $F(30,452) = 16.07, p < .0001; \Delta BIC_{4pair/2pair} = -176.59, Pr_{BIC}(2pair/Data) < .0001$ ), and LYS

( $F(30,452) = 7.73, p < .0001; \Delta BIC_{4pair/2pair} = -20.55, Pr_{BIC}(2pair/Data) < .0001$ ). This indicates that four pairs of mechanisms are necessary.

A more complex model with five pairs of mechanisms was also tested. The number of free parameters increased to 68. Model comparison statistics suggested no improvement from the 4-pair model to the 5-pair model for LL ( $F(21,931) = 0.29, p = .9994; \Delta BIC_{4pair/5pair} = -138.58, Pr_{BIC}(5pair/Data) < .0001$ ), CPY ( $F(21,431) = 0.08, p > .9999; \Delta BIC_{4pair/5pair} = -128.51, Pr_{BIC}(5pair/Data) < .0001$ ), and LYS ( $F(21,431) = 0.02, p > .9999; \Delta BIC_{4pair/5pair} = -130.02, Pr_{BIC}(5pair/Data) < .0001$ ). This indicates that four pairs of mechanisms are sufficient.

#### 4.9. Spectral sensitivity of the mechanisms

Table 1 shows the contrast sensitivities estimated by the model. Contrast sensitivity can be transformed into spectral sensitivity. The spectral sensitivity  $Se' = [Se'_L, Se'_M, Se'_S]$  and  $Se'_L = Se_L/L_{BG}$ , with  $Se'_M$  and  $Se'_S$  defined similarly.

Table 1  
*Contrast Sensitivity of the Three Observers*

Parameter	LL	CPY	LYS
$Se_{L1}, -Se_{L5}$	84.3419	62.6184	49.0328
$Se_{M1}, -Se_{M5}$	-79.0515	-78.7940	-83.3250
$Se_{S1}, -Se_{S5}$	-2.8796	-1.4487	-1.6910
$Se_{L2}, -Se_{L6}$	-4.2629	-11.1654	-22.9074
$Se_{M2}, -Se_{M6}$	-2.9066	-35.9792	-15.3130
$Se_{S2}, -Se_{S6}$	34.3552	29.9796	20.9394
$Se_{L3}, -Se_{L7}$	174.2947	197.9977	339.1530
$Se_{M3}, -Se_{M7}$	-29.0651	-29.2401	-32.0672
$Se_{S3}, -Se_{S7}$	13.1674	10.6912	11.1151
$Se_{L4}, -Se_{L8}$	122.3363	123.6739	118.2115
$Se_{M4}, -Se_{M8}$	-38.9724	-41.3714	-36.2792
$Se_{S4}, -Se_{S8}$	-15.2473	-14.9919	-9.3372

Taking spectral sensitivities with respect to three cone classes as the weightings to cone fundamentals gives the spectral sensitivity functions of the color mechanisms.

Figure 8 shows the spectral sensitivity functions of the four mechanisms normalized to peak values for the three observers and the averages across these observers. Each mechanism is one member in the opposite sign pair. The sensitivity functions of the other mechanisms are negative to those plotted in Figure 8. The cardinal equiluminant mechanisms (Guth et al., 1980) and luminosity efficiency functions representing the luminance mechanism (CIE, 2006) are plotted in dashed lines (2-degree eccentricity estimate) and dot lines (10-degree eccentricity estimate and only for luminosity function; almost overlapping with the 2-degree estimate) for comparison.

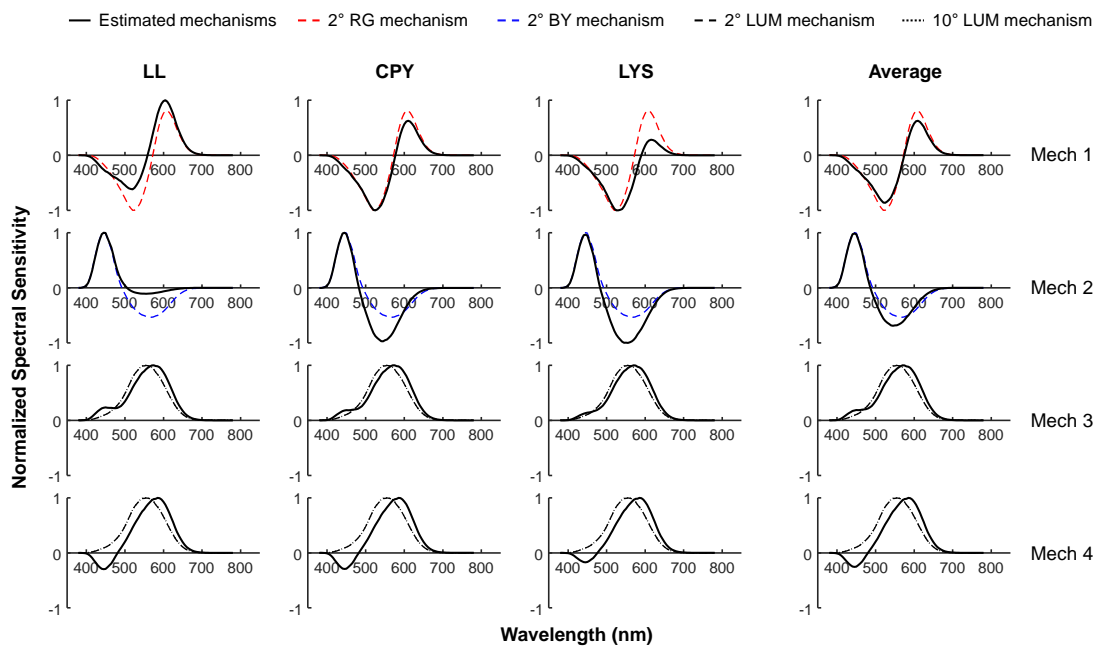


Figure 8. Spectral sensitivity functions of the estimated mechanisms for the three observers and the average. The black lines are the estimated sensitivity functions. The red and blue dashed lines plotted are the proposed red-green (RG) and blue-yellow (BY) mechanisms (Guth et al., 1980), respectively. The black dashed (2-degree eccentricity estimate) or dotted lines (10-degree eccentricity estimate; almost overlapping with the 2-degree estimate) are luminosity efficiency functions (CIE, 2006) that represent the luminance (LUM) mechanism.

The first mechanism mainly opposes the L cone to the M cone signal. The sensitivity has a peak at 615 nm and a trough at 525 nm. The second mechanism opposes the S cone signal to the sum of the L and M cone signals. The sensitivity of the second mechanism has a peak at 445 nm and a trough around 545 nm. The first and the second mechanisms correspond roughly to the proposed red-green and blue-yellow cardinal mechanisms.

The sensitivities of the third and the fourth mechanisms give large weights on the L-cone and relatively moderate amounts on the M-cone. The L and M cone weights are of opposite signs. The sensitivities peak at around 570 and 585 nm, respectively. Both mechanisms receive some signals from the S cone but one has positive input, whereas the other has negative input. These S cone inputs are stronger than that of the red-green (the first) mechanism, but weaker than that of the blue-yellow (the second) mechanism. Compared to the luminosity functions, their peaked sensitivities shift to longer wavelengths, and the shape of the sensitivity functions deviate at short to medium wavelength ranges. This suggests that they might not be the luminance mechanism. Instead, they may be better considered as intermediate mechanisms.

The model did not produce any luminance mechanism, even though we put no constraints on the shape of the sensitivity functions. This indicates that a luminance mechanism was not necessary to capture the systematic variations in our data.

#### **4.10. Comparisons to the literature**

Color mechanisms, in addition to the cardinal mechanisms, have been found in several research domains (Eskew, 2009), including perceptual grouping.

Previous studies have acknowledged the existence of multiple mechanisms at the local stage of perceptual grouping (Mandelli & Kiper, 2005; Wilson & Switkes, 2005). We also found that, with multiple ways of grouping, extra mechanisms are needed. We



have shown contrast sensitivity of the estimated mechanisms in Table 1. The cone contrast sensitivity vector for each mechanism represents the most sensitive direction of that mechanism in a color space. These contrast sensitivity vectors can be transformed into polar representations on the color space.

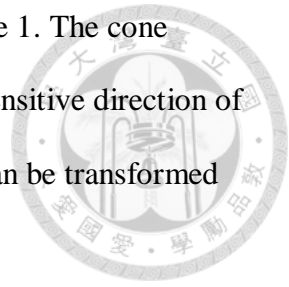
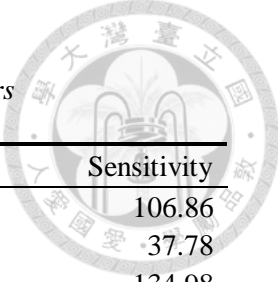


Table 2 shows the contrast sensitivity vectors in polar representation, in which the azimuth represents a polar angle relative to the L-M axis on the equiluminance plane, elevation represents the angle between the color vector and its projection onto the equiluminance plane, and sensitivity is the vector length. We have described the stimulus azimuth in a threshold-scaled color space (for S and L-M plane). The equivalent axis scaling to the color space representing mechanism sensitivity is the transposed inverse of the linear transformation done to the space representing the stimulus colors (Knoblauch & d'Zmura, 2001). Following this, the azimuth in the table are shown after scaling.

The azimuth of the estimated mechanisms correspond well to the intermediate mechanisms suggested in the literature (Mandelli & Kiper, 2005; Wilson & Switkes, 2005). The sensitivity vector of the luminance mechanism transformed to polar representation has an elevation of  $86.89^\circ$ . Non-zeroed elevations of the estimated mechanisms indicate that they contribute to luminance perception. However, they are far below the elevation of the luminance mechanism.

The color-spatial vision model has been applied in a pattern-masking paradigm (Chen et al., 2000a, 2000b). As discussed previously, the model was specific to local pattern detection with a fixed spatial frequency and orientation. Our model, instead, is designed for equiluminance pattern detection that involves the process of integrating local signals into a global form. Our study indicates that a modified model following Chen et al. (2000b) works well in perceptual grouping.

Table 2

*Polar Representation of the Estimated Mechanisms for the Three Observers*


Observer	Mechanism	Azimuth (°)	Elevation (°)	Sensitivity
LL	1	-10.74	0.75	106.86
	2	89.79	24.55	37.78
	3	43.27	42.66	134.98
	4	-51.29	24.25	95.77
CPY	1	-6.05	-5.95	98.15
	2	82.50	-13.55	42.31
	3	35.17	43.59	150.28
	4	-50.35	23.36	98.01
LYS	1	-11.96	-12.19	98.37
	2	88.98	-24.98	23.63
	3	38.35	47.31	249.98
	4	-53.95	26.98	92.41

*Note:* The azimuth represents a polar angle relative to the L-M axis on the equiluminance plane, elevation represents the angle between the color vector and its projection onto the equiluminance plane, and sensitivity is the vector length. Four of the mechanisms are listed in the table. These mechanisms are the same as those in Table 1. The other half of the mechanisms have a 180-degree difference in azimuth and elevation to those in the table. Azimuths are represented in the equal sensitivity mechanism space that is the dual space of a threshold-scaled stimulus space (Knoblauch & d'Zmura, 2001).

#### 4.11. The issue of subjective equiluminance

Luminosity efficiency function,  $V(\lambda)$ , is assumed to represent the spectral sensitivity of the postreceptoral luminance mechanism (Lennie, Pokorny, & Smith, 1993). A  $V(\lambda)$  curve results from a weighted combination of L and M cone signals. The relative weights of the two cone types differ from individual to individual (Bedford & Wyszecki, 1958; Ikeda, Yaguchi, & Sagawa, 1982). As a result, the plane that defines equiluminant inputs to the visual system varies among individuals. Many researchers have measured the subjective equiluminance and individualized color space for each observer in order to reduce the luminance artefact (Gunther, 2014; Kingdom, Kardous,

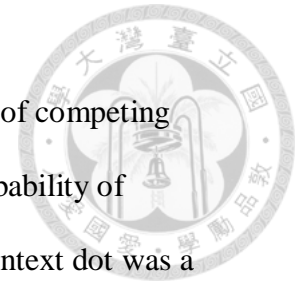
Curran, Gheorghiu, & Bell, 2014; Sato et al., 2020). This was done with techniques such as Heterochromatic Flicker Photometry (HFP), in which two colored patches were alternately presented in the same area in high temporal frequency, and the observer adjusted the relative luminance of the patches to minimize the flicker. The use of HFP and other similar techniques is based on the hypothesis that the equiluminance setting in HFP is similar to that in equiluminance pattern vision, which has not been directly examined by any study.

We chose stimulus color directions that were orthogonal to the direction of the CIE luminosity function (CIE, 2006). The CIE luminosity function represents the luminance mechanism of the standard observer but not individual observers. Therefore, the nominal equiluminant stimuli in our experiment might excite the luminance mechanism of the observers. However, we were able to take the luminance effect into account in our model. The estimated mechanisms were not restricted to lie on the nominal equiluminant plane. Instead, they could have luminance components. Whether these mechanisms have luminance components will not change the conclusion of this study.

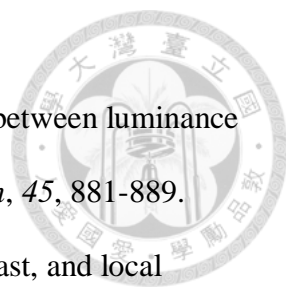
## 5. Conclusion

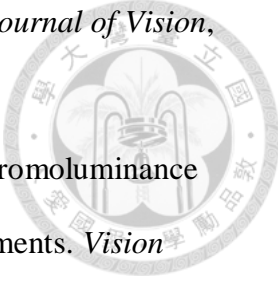
We investigated chromatic mechanisms in perceptual grouping of competing patterns varying in chromaticity and contrast. We found that the probability of perceiving the global pattern composed of the anchor dot and one context dot was a sigmoid-shape function of the context dot contrast. The probability function shifted in a downward right direction as the other context dot contrast increased. The probability change with the dot contrast of the respective patterns, indicating grouping competition. Regardless of the referenced chromaticity, the probability of grouping the anchor dot with the same color dots decreased when the chromaticity of the different color dot was closer to that of the anchor dot.

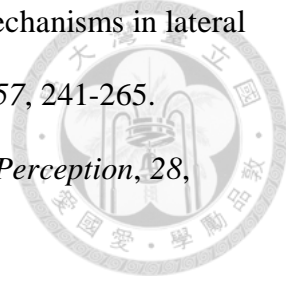
A divisive inhibition model with four pairs of chromatic mechanisms successfully explained the result. Spectral sensitivity functions of these mechanisms indicate that two pairs of these mechanisms are the red-green and blue-yellow cardinal mechanisms and the two other pairs are intermediate mechanisms. Our study indicates that perceptual grouping involves additional color mechanisms than those found at the previous stage of visual processing.




## 6. References

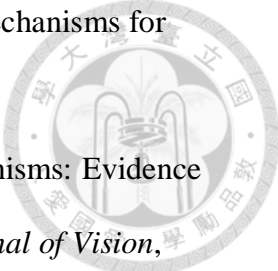
- 
- Badcock, D. R., Clifford, C. W., & Khuu, S. K. (2005). Interactions between luminance and contrast signals in global form detection. *Vision Research*, *45*, 881-889.
- Beaudot, W. H., & Mullen, K. T. (2000). Role of chromaticity, contrast, and local orientation cues in the perception of density. *Perception*, *29*, 581-600.
- Beaudot, W. H., & Mullen, K. T. (2001). Processing time of contour integration: The role of colour, contrast, and curvature. *Perception*, *30*, 833-853.
- Beaudot, W. H., & Mullen, K. T. (2003). How long range is contour integration in human color vision? *Visual Neuroscience*, *20*, 51-64.
- Bedford, R., & Wyszecki, G. W. (1958). Luminosity functions for various field sizes and levels of retinal illuminance. *Journal of the Optical Society of America*, *48*, 406-411.
- Brainard, D. (1996). Cone contrast and opponent modulation color spaces. In P. K. Kaiser & R. M. Boynton (Eds.), *Human color vision* (pp. 563-579). Washington, DC: Optical Society of America.
- Brainard, D. H. (1997). The psychophysics toolbox. *Spatial Vision*, *10*, 433-436.
- Carandini, M., Heeger, D. J., & Movshon, J. A. (1997). Linearity and normalization in simple cells of the macaque primary visual cortex. *Journal of Neuroscience*, *17*, 8621-8644.
- Carandini, M., Heeger, D. J., & Movshon, J. A. (1999). Linearity and gain control in V1 simple cells. In P. S. Ulinski, E. G. Jones, & A. E. Peters (Eds.), *Models of cortical circuits* (pp. 401-443). Boston, MA: Springer.
- Cardinal, K. S., & Kiper, D. C. (2003). The detection of colored Glass patterns. *Journal of Vision*, *3*, 199-208.

- 
- Chen, C.-C. (2009). A masking analysis of glass pattern perception. *Journal of Vision*, 9(12), 1-11.
- Chen, C.-C., Foley, J. M., & Brainard, D. H. (2000a). Detection of chromoluminance patterns on chromoluminance pedestals I: Threshold measurements. *Vision Research*, 40, 773-788. Retrieved from <https://www.ncbi.nlm.nih.gov/pubmed/10683455>
- Chen, C.-C., Foley, J. M., & Brainard, D. H. (2000b). Detection of chromoluminance patterns on chromoluminance pedestals II: model. *Vision Research*, 40, 789-803. Retrieved from <https://www.ncbi.nlm.nih.gov/pubmed/10683456>
- CIE. (2006). *Fundamental chromaticity diagram with physiological axes—Part 1, Technical Report 170-1:2006*. Vienna, Austria: International Commission on Illumination
- Clifford, C. W., Spehar, B., Solomon, S. G., Martin, P. R., & Qasim, Z. (2003). Interactions between color and luminance in the perception of orientation. *Journal of Vision*, 3, 106-115.
- D’Zmura, M., & Knoblauch, K. (1998). Spectral bandwidths for the detection of color. *Vision Research*, 38, 3117-3128.
- Dakin, S. C., & Bex, P. J. (2001). Local and global visual grouping: Tuning for spatial frequency and contrast. *Journal of Vision*, 1, 99-111.
- De Valois, R. L., Cottaris, N. P., Elfar, S. D., Mahon, L. E., & Wilson, J. A. (2000). Some transformations of color information from lateral geniculate nucleus to striate cortex. *Proceedings of the National Academy of Sciences*, 97, 4997-5002.
- De Valois, R. L., & De Valois, K. K. (1993). A multi-stage color model. *Vision Research*, 33, 1053-1065.

- 
- Derrington, A. M., Krauskopf, J., & Lennie, P. (1984). Chromatic mechanisms in lateral geniculate nucleus of macaque. *The Journal of Physiology*, *357*, 241-265.
- Earle, D. C. (1999). Glass patterns: Grouping by contrast similarity. *Perception*, *28*, 1373-1382.
- Ellenbogen, T., Polat, U., & Spitzer, H. (2006). Chromatic collinear facilitation, further evidence for chromatic form perception. *Spatial Vision*, *19*, 547-568. Retrieved from <https://www.ncbi.nlm.nih.gov/pubmed/17278527>
- Eskew, R. T. (2009). Higher order color mechanisms: A critical review. *Vision Research*, *49*, 2686-2704.
- Eskew, R. T., Stromeyer, C. F., Picotte, C. J., & Kronauer, R. E. (1991). Detection uncertainty and the facilitation of chromatic detection by luminance contours. *Journal of the Optical Society of America A*, *8*, 394-403.
- Eskew, R. T. J., Newton, J. R., & Giulianini, F. (2001). Chromatic detection and discrimination analyzed by a Bayesian classifier. *Vision Research*, *41*, 893-909.
- Flanagan, P., Cavanagh, P., & Favreau, O. E. (1990). Independent orientation-selective mechanisms for the cardinal directions of colour space. *Vision Research*, *30*, 769-778.
- Foley, J. M. (1994). Human luminance pattern-vision mechanisms: Masking experiments require a new model. *Journal of the Optical Society of America A*, *11*, 1710-1719.
- Freeman, T. C., Durand, S., Kiper, D. C., & Carandini, M. (2002). Suppression without inhibition in visual cortex. *Neuron*, *35*, 759-771.
- Friedman, H. S., Zhou, H., & von der Heydt, R. (2003). The coding of uniform colour figures in monkey visual cortex. *The Journal of Physiology*, *548*, 593-613.  
doi:10.1113/jphysiol.2002.033555

- 
- Gegenfurtner, K. R., & Kiper, D. C. (1992). Contrast detection in luminance and chromatic noise. *Journal of the Optical Society of America A*, 9, 1880-1888.
- Gegenfurtner, K. R., & Kiper, D. C. (2003). Color vision. *Annual Review of Neuroscience*, 26, 181-206.
- Geisler, W. S., & Albrecht, D. G. (1992). Cortical neurons: Isolation of contrast gain control. *Vision Research*, 32, 1409-1410.
- Giulianini, F., & Eskew, R. T. J. (1998). Chromatic masking in the ( $\Delta L/L$ ,  $\Delta M/M$ ) plane of cone-contrast space reveals only two detection mechanisms. *Vision Research*, 38, 3913-3926.
- Glass, L. (1969). Moire effect from random dots. *Nature*, 223, 578-580.
- Glass, L., & Pérez, R. (1973). Perception of random dot interference patterns. *Nature*, 246, 360-362.
- Glass, L., & Switkes, E. (1976). Pattern recognition in humans: Correlations which cannot be perceived. *Perception*, 5, 67-72.
- Gunther, K. L. (2014). Non-cardinal color perception across the retina: Easy for orange, hard for burgundy and sky blue. *Journal of the Optical Society of America A*, 31, A274-A282.
- Guth, S. L. (1991). Model for color vision and light adaptation. *Journal of the Optical Society of America A*, 8, 976-993.
- Guth, S. L., Massof, R. W., & Benzschawel, T. (1980). Vector model for normal and dichromatic color vision. *Journal of the Optical Society of America*, 70, 197-212.
- Hansen, T., & Gegenfurtner, K. R. (2005). Classification images for chromatic signal detection. *Journal of the Optical Society of America A*, 22, 2081-2089.



- 
- Hansen, T., & Gegenfurtner, K. R. (2006). Higher level chromatic mechanisms for image segmentation. *Journal of Vision*, 6, 239-259.
- Hansen, T., & Gegenfurtner, K. R. (2013). Higher order color mechanisms: Evidence from noise-masking experiments in cone contrast space. *Journal of Vision*, 13(1), 1-21.
- Hansen, T., & Gegenfurtner, K. R. (2017). Color contributes to object-contour perception in natural scenes. *Journal of Vision*, 17(3), 1-19.
- Huang, P. C., & Chen, C.-C. (2016). Contrast gain control in plaid pattern detection. *PLoS One*, 11(10), e0164171. doi:10.1371/journal.pone.0164171
- Huang, P. C., Mullen, K. T., & Hess, R. F. (2007). Collinear facilitation in color vision. *Journal of Vision*, 7(11), 1-14. doi:10.1167/7.11.6
- Hurvich, L. M., & Jameson, D. (1957). An opponent-process theory of color vision. *Psychological Review*, 64(6), 384-404.
- Ikeda, M., Yaguchi, H., & Sagawa, K. (1982). Brightness luminous-efficiency functions for 2° and 10° fields. *Journal of the Optical Society of America*, 72, 1660-1665.
- Kingdom, F. A., Kardous, N., Curran, L., Gheorghiu, E., & Bell, J. (2014). Saliency interactions between the 'L-M' and 'S' cardinal colour directions. *Vision Research*, 95, 36-42.
- Kiper, D. C., Fenstemaker, S. B., & Gegenfurtner, K. R. (1997). Chromatic properties of neurons in macaque area V2. *Visual Neuroscience*, 14, 1061-1072. Retrieved from <https://www.ncbi.nlm.nih.gov/pubmed/9447688>
- Kleiner, M., Brainard, D., & Pelli, D. (2007). What's new in Psychtoolbox-3? *Perception*, 36(14), 1-16.
- Knoblauch, K., & d'Zmura, M. (2001). Reply to letter to editor by MJ Sankeralli and KT Mullen published in *Vision Research*, 41, 53-55: Lights and neural

responses do not depend on choice of color space. *Vision Research*, *41*, 1683-1684.



Koffka, K. (1963). *Principles of Gestalt psychology*. New York: Harcourt, Brace & World. (Original work published in 1935)

Krauskopf, J., Williams, D. R., & Heeley, D. W. (1982). Cardinal directions of color space. *Vision Research*, *22*, 1123-1131.

Kurki, I., Laurinen, P., Peromaa, T., & Saarinen, J. (2003). Spatial integration in Glass patterns. *Perception*, *32*, 1211-1220.

Lennie, P., Pokorny, J., & Smith, V. C. (1993). Luminance. *Journal of the Optical Society of America A*, *10*, 1283-1293.

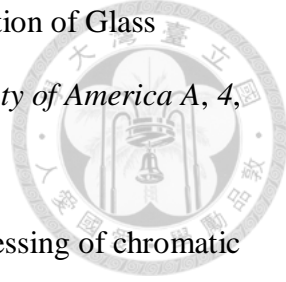
Lin, Y.-S. (2016). *The role of color contrast gain control in global form perception*. (Unpublished master's thesis). National Taiwan University, Taipei, Taiwan.

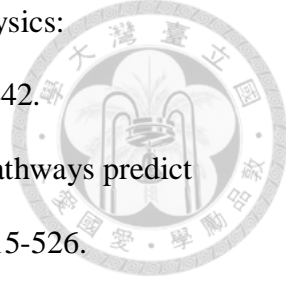
Lin, Y.-S., Cho, P.-C., & Chen, C.-C. (2017). Contrast gain control determines global form percept in tripole Glass patterns. *Journal of Vision*, *17*(5), 1-9.

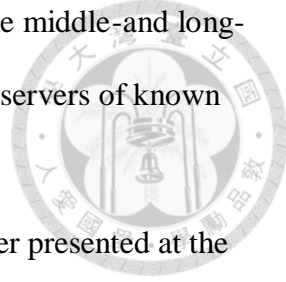
Livingstone, M., & Hubel, D. (1988). Segregation of form, color, movement, and depth: anatomy, physiology, and perception. *Science*, *240*, 740-749.  
doi:10.1126/science.3283936

Livingstone, M. S., & Hubel, D. H. (1987). Psychophysical evidence for separate channels for the perception of form, color, movement, and depth. *Journal of Neuroscience*, *7*, 3416-3468. Retrieved from <https://www.ncbi.nlm.nih.gov/pubmed/3316524>

MacLeod, D. I., & Boynton, R. M. (1979). Chromaticity diagram showing cone excitation by stimuli of equal luminance. *Journal of the Optical Society of America*, *69*, 1183-1186.

- 
- Maloney, R., Mitchison, G., & Barlow, H. (1987). Limit to the detection of Glass patterns in the presence of noise. *Journal of the Optical Society of America A*, 4, 2336-2341.
- Mandelli, M.-J. F., & Kiper, D. C. (2005). The local and global processing of chromatic Glass patterns. *Journal of Vision*, 5, 405-416.
- McIlhagga, W. H., & Mullen, K. T. (1996). Contour integration with colour and luminance contrast. *Vision Research*, 36, 1265-1279.
- Moutoussis, K. (2015). The physiology and psychophysics of the color-form relationship: A review. *Frontiers in Psychology*, 6, 1407.
- Mullen, K. T., & Beaudot, W. H. (2002). Comparison of color and luminance vision on a global shape discrimination task. *Vision Research*, 42, 565-575.
- Mullen, K. T., Beaudot, W. H., & McIlhagga, W. H. (2000). Contour integration in color vision: A common process for the blue–yellow, red–green and luminance mechanisms? *Vision Research*, 40, 639-655.
- Mullen, K. T., & Losada, M. A. (1994). Evidence for separate pathways for color and luminance detection mechanisms. *Journal of the Optical Society of America A*, 11, 3136-3151.
- Mullen, K. T., & Sankeralli, M. J. (1999). Evidence for the stochastic independence of the blue-yellow, red-green and luminance detection mechanisms revealed by subthreshold summation. *Vision Research*, 39, 733-745.
- Ohzawa, I., Sclar, G., & Freeman, R. D. (1982). Contrast gain control in the cat visual cortex. *Nature*, 298, 266-268. doi:10.1038/298266a0
- Ohzawa, I., Sclar, G., & Freeman, R. D. (1985). Contrast gain control in the cat's visual system. *Journal of Neurophysiology*, 54, 651-667. doi:10.1152/jn.1985.54.3.651

- 
- Pelli, D. G. (1997). The VideoToolbox software for visual psychophysics: Transforming numbers into movies. *Spatial Vision*, *10*, 437-442.
- Poirson, A. B., & Wandell, B. A. (1996). Pattern—color separable pathways predict sensitivity to simple colored patterns. *Vision Research*, *36*, 515-526.
- Poirson, A. B., Wandell, B. A., Varner, D. C., & Brainard, D. H. (1990). Surface characterizations of color thresholds. *Journal of the Optical Society of America A*, *7*, 783-789.
- Prazdny, K. (1986). Some new phenomena in the perception of Glass patterns. *Biological Cybernetics*, *53*, 153-158.
- Quick, R. (1974). A vector-magnitude model of contrast detection. *Kybernetik*, *16*, 65-67.
- Quinlan, P. T., & Wilton, R. N. (1998). Grouping by proximity or similarity? Competition between the Gestalt principles in vision. *Perception*, *27*, 417-430.
- Reid, R. C., & Shapley, R. M. (2002). Space and time maps of cone photoreceptor signals in macaque lateral geniculate nucleus. *Journal of Neuroscience*, *22*, 6158-6175.
- Sankeralli, M. J., & Mullen, K. T. (1997). Postreceptoral chromatic detection mechanisms revealed by noise masking in three-dimensional cone contrast space. *Journal of the Optical Society of America A*, *14*, 2633-2646.
- Sankeralli, M. J., & Mullen, K. T. (2001). Assumptions concerning orthogonality in threshold-scaled versus cone-contrast colour spaces. *Vision Research*, *41*, 53-55.
- Sato, T., Nagai, T., & Kuriki, I. (2020). Hue selectivity of collinear facilitation. *Journal of the Optical Society of America A*, *37*, A154-A162.
- Shapley, R., & Hawken, M. J. (2011). Color in the cortex: single- and double-opponent cells. *Vision Research*, *51*, 701-717. doi:10.1016/j.visres.2011.02.012

- 
- Stockman, A., & Sharpe, L. T. (2000). The spectral sensitivities of the middle-and long-wavelength-sensitive cones derived from measurements in observers of known genotype. *Vision Research*, *40*, 1711-1737.
- Teo, P. C., & Heeger, D. J. (1994). *Perceptual image distortion*. Paper presented at the Proceedings of 1st International Conference on Image Processing, Austin, TX, USA.
- Watanabe, A., Smith, V., & Pokorny, J. (1997). Psychometric functions for chromatic discriminations. In C. R. Cavonius (Ed.), *Colour vision deficiencies XIII* (pp. 369-376). Dordrecht, The Netherlands: Kluwer Academic Publishers.
- Watson, A. B., & Solomon, J. A. (1997). Model of visual contrast gain control and pattern masking. *Journal of the Optical Society of America A*, *14*, 2379-2391.
- Webster, M. A., De Valois, K. K., & Switkes, E. (1990). Orientation and spatial-frequency discrimination for luminance and chromatic gratings. *Journal of the Optical Society of America A*, *7*, 1034-1049.
- Webster, M. A., & Mollon, J. (1994). The influence of contrast adaptation on color appearance. *Vision Research*, *34*, 1993-2020.
- Wertheimer, M. (1938). Untersuchungen zur Lehre von der Gestalt, II [Investigations of the principles of gestalt II]. Translation published in W. D. Ellis (Ed.), *A source book of gestalt psychology* (pp. 71-88). London, UK: Routledge & Kegan Paul. (Reprinted from *Psychologische Forschung*, *4*, 301-350, 1923)
- Wilson, H. R., & Wilkinson, F. (1998). Detection of global structure in Glass patterns: Implications for form vision. *Vision Research*, *38*, 2933-2947.
- Wilson, H. R., Wilkinson, F., & Asaad, W. (1997). Concentric orientation summation in human form vision. *Vision Research*, *37*, 2325-2330.

Wilson, J. A., & Switkes, E. (2005). Integration of differing chromaticities in early and midlevel spatial vision. *Journal of the Optical Society of America A*, 22, 2169-2181.

Wilson, J. A., Switkes, E., & De Valois, R. L. (2004). Glass pattern studies of local and global processing of contrast variations. *Vision Research*, 44, 2629-2641.  
doi:10.1016/j.visres.2003.06.001

Zaidi, Q., & Halevy, D. (1993). Visual mechanisms that signal the direction of color changes. *Vision Research*, 33, 1037-1051.

Zeki, S., & Shipp, S. (1988). The functional logic of cortical connections. *Nature*, 335, 311-317. doi:10.1038/335311a0

## Appendix A: Detection Threshold Measurement

Detectability of dipole Glass patterns was tested with at least 4 color directions for each observer. Method of constant stimuli was used. The observer reported the orientation of the spiral pattern (clockwise or counterclockwise) during the task.

Accuracy against color contrast was fitted with a cumulative Gaussian function. Contrast strength corresponding to 75% accuracy was chosen to be the detection threshold. All threshold points were then fitted with an ellipse (Poirson & Wandell, 1996; Poirson, Wandell, Varner, & Brainard, 1990). This ellipse gave the equal threshold contour on the equiluminant plane.

The aspect ratio of the ellipse was used to normalize the cardinal equiluminant axes. The intermediate color directions was defined after the scaling. The normalized cone contrast vectors of the intermediate directions as well as the cardinal directions are given in Table A1. Stimuli strength was set to threshold multiples of a given color direction.

Table A1

*Normalized Cone Contrast Vectors for the Three Observers*

	Cardinal direction		Intermediate direction					
	0°/180°	90°/270°	LL		CPY		LYS	
	0°/180°	90°/270°	45°/225°	135°/315°	45°/225°	135°/315°	45°/225°	135°/315°
L	±0.4126	0	±0.0580	∓0.0580	±0.0572	∓0.0572	±0.0342	∓0.0342
M	∓0.9109	0	∓0.1281	±0.1281	∓0.1264	±0.1264	∓0.0755	±0.0755
S	0	±1.0000	±0.9901	±0.9901	±0.9903	±0.9903	±0.9966	±0.9966

## Appendix B: Symbols Used in the Quantitative Description of the Model



Table A2

*Symbols Used in the Quantitative Description of the Model*

Symbol	Description
$C_1 = [C_{L1}, C_{M1}, C_{S1}]^T$ and $C_2 = [C_{L2}, C_{M2}, C_{S2}]^T$	Cone contrast vector with three entries specifying the LMS cone contrast of the two dots.
$G_j = [G_{Lj}, G_{Mj}, G_{Sj}]^T$	Contrast gain vector of the local color-spatial operator with $j^{th}$ chromatic mechanism.
$Se_j = [Se_{Lj}, Se_{Mj}, Se_{Sj}]^T$	Contrast sensitivity vector of the global detector with $j^{th}$ chromatic mechanism.
$I_1(x,y)$ and $I_2(x,y)$	Spatial modulation of the two dots.
$f(\Delta x, \Delta y)$	Spatial profile of the operator. $\Delta x = x - x_0$ and $\Delta y = y - y_0$ , where $x_0$ and $y_0$ specify the midpoint between two dots.
$Ed'_j$	Excitation of the local color-spatial operator with $j^{th}$ chromatic mechanism.
$E'_j$	Excitation of the global detector with $j^{th}$ chromatic mechanism.
$E'_{j,\rho}$	Excitation of the global detector with $j^{th}$ chromatic mechanism and $\rho$ preferred pattern orientation.
$E_{j,\rho}$	Half-wave rectified excitation of the global detector with $j^{th}$ chromatic mechanism and $\rho$ preferred pattern orientation.
$Si_{ij,\rho'}$	Inhibitory weight for the inhibition from the detector with the $i^{th}$ chromatic mechanism and $\rho'$ pattern orientation to the detector with the $j^{th}$ chromatic mechanism and $\rho$ pattern orientation.
$I_{j,\rho}$	Total inhibition to the global detector with $j^{th}$ chromatic mechanism and $\rho$ preferred pattern orientation.
$R_{j,\rho}$	Response of the detector with $j^{th}$ chromatic mechanism with $\rho$ preferred pattern orientation.
$R_\rho$	Combined detector response from all chromatic mechanisms with $\rho$ preferred pattern orientation.
$D$	Decision variable.



## Appendix C. Best-fitted Model Parameter List

Table A3 lists all parameters of the best-fitted model for the three observers. The model contained eight, or four pairs of, mechanisms denoted by the subscript number (1 to 4 for different chromatic mechanisms and 5 to 8 as their opposite sign counterparts).

Table A3

### *Best-fitted Model Parameters*

Parameter	LL	CPY	LYS
Se <sub>L1</sub> , -Se <sub>L5</sub>	84.3419	62.6184	49.0328
Se <sub>M1</sub> , -Se <sub>M5</sub>	-79.0515	-78.7940	-83.3250
Se <sub>S1</sub> , -Se <sub>S5</sub>	-2.8796	-1.4487	-1.6910
Se <sub>L2</sub> , -Se <sub>L6</sub>	-4.2629	-11.1654	-22.9074
Se <sub>M2</sub> , -Se <sub>M6</sub>	-2.9066	-35.9792	-15.3130
Se <sub>S2</sub> , -Se <sub>S6</sub>	34.3552	29.9796	20.9394
Se <sub>L3</sub> , -Se <sub>L7</sub>	174.2947	197.9977	339.1530
Se <sub>M3</sub> , -Se <sub>M7</sub>	-29.0651	-29.2401	-32.0672
Se <sub>S3</sub> , -Se <sub>S7</sub>	13.1674	10.6912	11.1151
Se <sub>L4</sub> , -Se <sub>L8</sub>	122.3363	123.6739	118.2115
Se <sub>M4</sub> , -Se <sub>M8</sub>	-38.9724	-41.3714	-36.2792
Se <sub>S4</sub> , -Se <sub>S8</sub>	-15.2473	-14.9919	-9.3372
SiS <sub>11</sub> , SiS <sub>55</sub> , SiS <sub>15</sub> , SiS <sub>51</sub>	0.1590	0.4863	0.4404
SiS <sub>12</sub> , SiS <sub>56</sub> , SiS <sub>16</sub> , SiS <sub>52</sub>	1.2279	0.0848	1.4764
SiS <sub>13</sub> , SiS <sub>57</sub> , SiS <sub>17</sub> , SiS <sub>53</sub>	0.4001	0.7148	1.2765
SiS <sub>14</sub> , SiS <sub>58</sub> , SiS <sub>18</sub> , SiS <sub>54</sub>	0.3633	0.8684	0.7185
SiS <sub>21</sub> , SiS <sub>65</sub> , SiS <sub>25</sub> , SiS <sub>61</sub>	0.2028	0.0060	0.4883
SiS <sub>22</sub> , SiS <sub>66</sub> , SiS <sub>26</sub> , SiS <sub>62</sub>	0.3045	0.4577	0.5799
SiS <sub>23</sub> , SiS <sub>67</sub> , SiS <sub>27</sub> , SiS <sub>63</sub>	0.1814	0.2364	0.5804
SiS <sub>24</sub> , SiS <sub>68</sub> , SiS <sub>28</sub> , SiS <sub>64</sub>	0.1377	0.2385	0.4927
SiS <sub>31</sub> , SiS <sub>75</sub> , SiS <sub>35</sub> , SiS <sub>71</sub>	0.3187	0.2669	0.3470
SiS <sub>32</sub> , SiS <sub>76</sub> , SiS <sub>36</sub> , SiS <sub>72</sub>	0.6375	1.0491	0.7537
SiS <sub>33</sub> , SiS <sub>77</sub> , SiS <sub>37</sub> , SiS <sub>73</sub>	0.3282	0.4927	0.5631
SiS <sub>34</sub> , SiS <sub>78</sub> , SiS <sub>38</sub> , SiS <sub>74</sub>	0.5195	0.6170	0.6142
SiS <sub>41</sub> , SiS <sub>85</sub> , SiS <sub>45</sub> , SiS <sub>81</sub>	0.3464	0.2415	0.5314
SiS <sub>42</sub> , SiS <sub>86</sub> , SiS <sub>46</sub> , SiS <sub>82</sub>	0.5254	0.8668	0.9913
SiS <sub>43</sub> , SiS <sub>87</sub> , SiS <sub>47</sub> , SiS <sub>83</sub>	0.3034	0.3018	1.4252
SiS <sub>44</sub> , SiS <sub>88</sub> , SiS <sub>48</sub> , SiS <sub>84</sub>	0.3339	0.4237	0.3442

(Continued.)

Table A3. (Continued.)

SiD <sub>11</sub> , SiD <sub>55</sub> , SiD <sub>15</sub> , SiD <sub>51</sub>	0.3076	0.4990	0.5520
SiD <sub>12</sub> , SiD <sub>56</sub> , SiD <sub>16</sub> , SiD <sub>52</sub>	0.0012	0.1507	0.4789
SiD <sub>13</sub> , SiD <sub>57</sub> , SiD <sub>17</sub> , SiD <sub>53</sub>	0.0038	0.0126	0.6353
SiD <sub>14</sub> , SiD <sub>58</sub> , SiD <sub>18</sub> , SiD <sub>54</sub>	0.0254	0.0034	0.5449
SiD <sub>21</sub> , SiD <sub>65</sub> , SiD <sub>25</sub> , SiD <sub>61</sub>	0.0005	0.0067	0.0013
SiD <sub>22</sub> , SiD <sub>66</sub> , SiD <sub>26</sub> , SiD <sub>62</sub>	0.3147	0.4242	0.5209
SiD <sub>23</sub> , SiD <sub>67</sub> , SiD <sub>27</sub> , SiD <sub>63</sub>	0.1103	0.0176	0.2649
SiD <sub>24</sub> , SiD <sub>68</sub> , SiD <sub>28</sub> , SiD <sub>64</sub>	0.1032	0.1371	0.0003
SiD <sub>31</sub> , SiD <sub>75</sub> , SiD <sub>35</sub> , SiD <sub>71</sub>	0.1285	0.1822	0.0002
SiD <sub>32</sub> , SiD <sub>76</sub> , SiD <sub>36</sub> , SiD <sub>72</sub>	0.1645	0.0129	0.2479
SiD <sub>33</sub> , SiD <sub>77</sub> , SiD <sub>37</sub> , SiD <sub>73</sub>	0.2729	0.4943	0.5027
SiD <sub>34</sub> , SiD <sub>78</sub> , SiD <sub>38</sub> , SiD <sub>74</sub>	0.0006	0.0061	0.0004
SiD <sub>41</sub> , SiD <sub>85</sub> , SiD <sub>45</sub> , SiD <sub>81</sub>	0.0040	0.2012	0.0026
SiD <sub>42</sub> , SiD <sub>86</sub> , SiD <sub>46</sub> , SiD <sub>82</sub>	0.0003	0.0036	0.0048
SiD <sub>43</sub> , SiD <sub>87</sub> , SiD <sub>47</sub> , SiD <sub>83</sub>	0.0009	0.1773	0.0727
SiD <sub>44</sub> , SiD <sub>88</sub> , SiD <sub>48</sub> , SiD <sub>84</sub>	0.2902	0.5199	0.4975
z	25.6819	193.3913	0.2209
p	2.5715	3.1609	2.9826
q	2.9289	3.5450	2.9715
m	2*	2*	2*
Mean(SE)	0.0408	0.0544	0.0580
RMSE	0.0608	0.0646	0.0640
R <sup>2</sup>	.9682	.9500	.9465

Note: Asterisks (\*) mark the fixed parameters.